Title
The use of HYDRUS-2D to simulate intermittent Agricultural Managed Aquifer Recharge (Ag-MAR) in Alfalfa in the San Joaquin Valley

Authors
Bali, Khaled M
Mohamed, Abdelmoneim Zakaria
Begna
et al.

Publication Date
2023-05-01

DOI
10.1016/j.agwat.2023.108296

The Use of HYDRUS-2D to Simulate Intermittent Agricultural Managed Aquifer Recharge (Ag-MAR) in Alfalfa in the San Joaquin Valley

Khaled M. Bali[1], Abdelmoneim Zakaria Mohamed[1], Sultan Begna[2], Dong Wang[2], Daniel Putnam[3], Helen E. Dahlke[4], Mohamed Galal Eltarabily[4,5*]

[1] UC Kearney Agricultural Research and Extension Center, University of California, Parlier, CA 93648, USA

[2] Water Management Research Unit. USDA-ARS, Parlier, CA 93648, USA

[3] Department of Plant Sciences, University of California, Davis, CA 95616, USA

[4] Department of Land, Air and Water Resources, University of California, Davis, CA 95616, USA

[5] Civil Engineering Department, Faculty of Engineering, Port Said University, Port Said 42523, Egypt

Emails: (Bali K.M.): kmbali@ucanr.edu & (Mohamed A.Z.): amohamed@ucdavis.edu & (Begna S.): Sultan.Begna@usda.gov & (Wang D.): dong.wang@usda.gov & (Putnam D.): dhputnam@ucdavis.edu & (Dahlke H.E.): hdahlke@ucdavis.edu & (Eltarabily M.G.): eng_m_trabily@eng.psu.edu.eg & meltarabily@ucdavis.edu

Abstract

Agricultural Managed Aquifer Recharge (Ag-MAR) is a potential and sustainable practice where agricultural fields can be used to recharge depleted aquifers using excess precipitation during winter. However, there is little information on the amount of Ag-MAR that can be applied to crops such as alfalfa. HYDRUS-2D was used to estimate the net recharge in an alfalfa field grown on a sandy loam soil in a Mediterranean climate at Parlier, California, USA in 2020–2022. The alfalfa field had four irrigation treatments: full irrigation during summer growing season (March through November), mid-summer deficit irrigation treatment (March to August and complete irrigation cutoff after August cutting), winter flooding treatment, and no winter flooding. Recharge, evapotranspiration (ET_a), soil moisture dynamics, and root water uptake were simulated during the recharge period in winter. Previously fully irrigated treatments in summer, followed by winter recharge led to cumulative groundwater recharge of 1459, 1687, and 1415 mm for 2020, 2021, and 2022, respectively. These applications resulted in a net recharge of 85, 89, and 84% of the applied irrigation water during the winter period, a significant contribution to groundwater aquifers. Mid-summer deficit irrigation treatments, followed by winter recharge, resulted in net groundwater recharge of 1337, 1498, and 1272 mm for 2020, 2021, and 2022, respectively, amounting to 78, 79, and 76% of the applied irrigation water during winter flooding periods. HYDRUS simulation model predicted groundwater recharge potential in these experiments successfully with a coefficient of determination, R^2 values of 0.91, and 0.89 for the groundwater recharge during winter flooding after the full irrigation in summer, and the mid-summer deficit irrigation, respectively. These results confirm the potential utilization of HYDRUS simulations in predicting groundwater recharge potential under similar sandy-soil conditions in California's San Joaquin Valley.

Keywords: Winter flooding; Agricultural Managed Aquifer Recharge; Alfalfa (Medicago sativa); Intermittent Groundwater Recharge; HYDRUS-2D

1. Introduction

Groundwater is one of the main sources of water for irrigation in California (CA), particularly during drought years (Dahlke *et al*., 2018). Groundwater pumping for agricultural water needs in CA is approximately 30% in wet years and increases up to 60% in dry years (Hanak *et al*., 2017). The recurring drought in CA has significantly increased groundwater pumping that exceeds the natural recharge rates (USGS, 2014; Lund, 2018). Additional depletion in groundwater aquifers will likely occur without considerable improvements in groundwater resource management in California (Alam *et al*., 2019). This is also relevant to other regions with similar agroecosystems and groundwater depletion history.

With the passage of the Sustainable Groundwater Management Act (SGMA) in 2014, Groundwater Sustainability Agencies (GSA) are actively exploring options for bringing the critically over-drafted basins back to their balance by 2040 (https://water.ca.gov/programs/groundwater-management/sgma-groundwater-management). The San Joaquin Valley of California is one of the most productive agricultural regions in the world, and it has several critically over-drafted basins under SGMA (DWR, 2016). The recent droughts in California have caused declines in groundwater levels in 90% of wells in the Central Valley of California which includes the San Joaquin Valley by as much as 3-15 m (DWR, 2017). These over-drafted basins could be brought back to balance by intentionally applying excess flood water on agricultural fields during the offseason (rainy season) for recharging aquifers (Jasechko and Perrone, 2020).

Agricultural Managed Aquifer Recharge (Ag-MAR) is an emerging technique that uses agricultural fields as percolation basins to recharge the underlying aquifers (Ganot and Dahlke, 2021 a). Ag-MAR refers to the cropland areas that can capture the excess water flow during winter to deliberately recharge groundwater (Kocis and Dahlke, 2017; Dahlke *et al*., 2018). Ag-MAR has been proposed for CA and could be an effective and potentially sustainable practice to bank excess water for long-term health of aquifers (Niswonger *et al*., 2017). Using high-quality surface water Ag-MAR could also decrease groundwater salinity over time in addition to decreasing pumping costs due to the rise in the water table (Bachand *et al*., 2014). The benefits and limitations of implementing Ag-MAR projects have been summarized by Levintal *et al*. (2022).

Alfalfa is grown on about 240,000 ha of 461,000 ha of total hay crops, including grasses in the San Joaquin Valley over the past 5 years (NASS, 2022). Given that a large percentage (~80%) of California alfalfa is flood-irrigated utilizing gravity-fed systems, alfalfa is an important candidate for Ag-MAR flooding (Putnam *et al*., 2021). On-farm groundwater recharge on alfalfa fields utilizing the existing surface irrigation infrastructures and excess surface water during high winter flows could be a promising water-saving practice for the longevity and sustainability of groundwater resources. Unlike the potential risks of leaching of residual pesticides or fertilizer in annual crops or fallow fields, alfalfa may be an ideal crop for Ag-MAR projects since it does not require any nitrogen fertilizer after establishment, obtaining all N needs from biological N_2 fixation or root uptake (Putnam *et al.*, 2015). Its deep-rooted system typically prevents movement of nitrates beyond the root zone and into the groundwater (Putnam and Lin, 2016). It should be noted that alfalfa is not considered to be highly flooding-tolerant, and sustained flooding on established stands, especially under hot conditions can kill plants and damage stands, primarily due to lack of soil oxygen, but also soil pathogens. Damage is primarily a function of length of the flooding season, whether the crop is dormant, temperature, soil physical properties, alfalfa varieties, and other factors. Tolerance to several weeks of flooding by pastures has been observed (Redfearn and Beckman, 2019). Moreover, recent studies on Ag-MAR on alfalfa have shown no significant negative impact on root health in soils with high percolation rates, provided soil oxygen deficits are avoided (Dahlke *et al.*, 2018).

There are many soil and agronomic parameters to be considered for successful implementation of Ag-MAR recharge projects. So, ideally, flooding for Ag-MAR is preferably done on fallow fields or during crop dormancy periods when agricultural fields have the potential to serve as percolation basins for groundwater recharge (Ganot and Dahlke, 2021 a). A tool for understanding ideal soils conditions, the soil-agricultural-groundwater banking index (SAGBI), has been developed (O'Geen *et al.*, 2015). Critical factors include soil deep percolation rate, root zone residence time, topography, chemical limitations, and soil surface conditions. Deep percolation rate and root zone residence time are frequently the most important factors, due to their important relevance to the amount of groundwater recharge. The commonly used approaches to quantify the potential for groundwater recharge and their associated limitations were summarized by Scanlon *et al*. (2002). Various methods have been recommended for using and accurately estimating the potential for groundwater recharge (Zhang *et al.*, 2020).

Numerical simulation models are essential to study newly developed groundwater recharge practices such as Ag-MAR. The HYDRUS software has been used in many studies to simulate vadose zone hydrologic processes, nutrient leaching, salinization, and plant growth in different soils. HYDRUS solves Richards equation (Šimůnek *et al.*, 1996) and has been widely used to simulate water flow and solute transport within the vadose zone. It is also used to quantify the recharge/discharge to/from groundwater (e.g., Eltarabily *et al.*, 2019 a, b, 2021). HYDRUS has been increasingly used to simulate groundwater recharge during the growing season from irrigated cropland regions (e.g., Jiménez-Martínez *et al.*, 2009; Lu *et al.*, 2011; Poch-Massegú *et al.*, 2014; Šimůnek, 2015; Patle *et al.*, 2017; Porhemmat *et al.*, 2018; Li *et al.*, 2019;

Dadgar *et al*., 2020; Li, 2020; Wang *et al*., 2021; Ganot and Dahlke, 2021b; Stafford *et al*., 2022; Post *et al*., 2022).

During the alfalfa growing season, the objective of irrigation is to achieve the highest yields and highest irrigation application efficiency while meeting crop evapotranspiration needs, with minimal deep percolation and surface runoff. However, during winter flooding, existing surface irrigation systems could be utilized to achieve pre-irrigation for crop production, as well as higher groundwater recharge efficiency while eliminating surface runoff, and providing minimal crop damage (due to poor soil aeration). Accurate predictions of groundwater recharge could help stakeholders and policymakers in making sustainable water resources management decisions. Thus, the objective of this study was to experimentally and numerically quantify the amount of applied water going to groundwater recharge on an alfalfa field utilizing an intermittent irrigation regime (one or two irrigation events per week) for Ag-MAR in the winter. This strategy was assessed under the combination of two summer irrigation treatments (full irrigation, and mid-summer deficit irrigation) using the soil water balance and HYDRUS-2D model. The results of this research could help in assessing the potential of utilizing Ag-MAR in the San Joaquin Valley of California for maintaining a sustainable management plan for groundwater resources.

2. Materials and Methods

2.1. Experimental Layout and Field Description

A field experiment was conducted at the University of California, Kearney Agricultural Research and Extension Center (KARE) near Parlier, CA in 2020–2022 on a one-year-old alfalfa field established in 2019 to determine the feasibility of utilizing the existing surface irrigation system for intermittent groundwater recharge and to quantify the potential depth of groundwater recharge during the alfalfa dormant growing period (winter season). The soil at the experimental site is classified as Hanford sandy loam (coarse-loamy, mixed, superactive, nonacid, thermic Typic Xerorthents), a well-drained soil with a very low runoff risk (hydrological soil group A). The landform is floodplains and alluvial fans. The parent material is Alluvium derived from granite. The slope is from 0 to 2 % (https://websoilsurvey.sc.egov.usda.gov/App/WebSoilSurvey.aspx). The depth to the water table at the study site was 27 m at the beginning of the experiment.

The experiment was conducted on a 1.51-hectare field that was divided into 12 checks/plots. Winter flood treatments were implemented on 50% of the total area (checks 1, 4, 5, 8, 9, and 12) (Fig. 1) while the other half of the field was not exposed to winter flooding (checks 2, 3, 6, 7, 10, and 11). Two irrigation treatments were applied during the growing season: full season-long irrigation (March through November), and mid-summer deficit irrigation treatment (irrigated only March through August). The fully irrigated plots received two flood irrigation events per cut during the whole growing season (March-November) and the mid-summer deficit irrigation plots were fully irrigated until early August and then irrigation was terminated after the August cutting. The irrigation treatments were replicated in three blocks and were designed to study the carry-over effect of the mid-summer deficit irrigation compared to full irrigation in summer on the net amount of groundwater recharge.

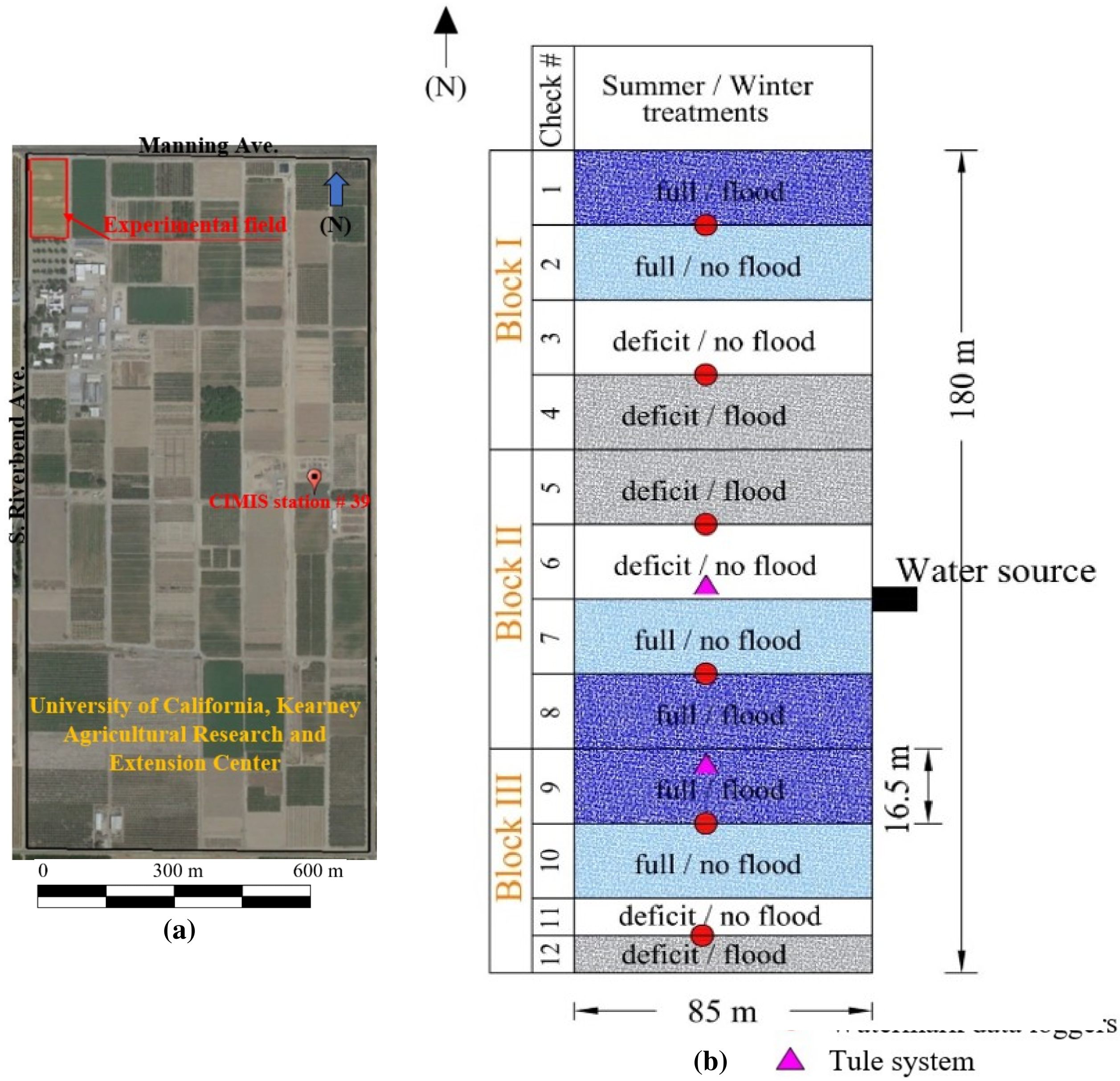

Note: Watermarks of two neighboring checks are connected to one data logger.

Treatments		Description
Summer	Winter	
Full	No Flood	Fully irrigated in summer and no winter flooding
Full	Flood	Fully irrigated in summer and winter flooding
Deficit	No Flood	August cutoff and no winter flooding
Deficit	Flood	August cutoff and winter flooding

Fig 1. **(a)** Keymap of the research center **(b)** Experimental layout with a randomized complete block design consisting of two summer treatments and two flooding treatments with three replicates, numbers represent the checks/plots (twelve in total, width 16.5 m wide by 85 m long for all checks, except for checks 11, and 12, both checks were 8.25 m wide and same length as the other checks)

2.2. Climate Data, Evapotranspiration, and Precipitation

Climatic data were acquired from the California Irrigation Management Information System (CIMIS) (CIMIS station no. 39) which is located at KARE (36º 35' 51" N, 119º 30' 15" W) (https://cimis.water.ca.gov/ Stations.aspx), and selected data are reported during the experimental period (Fig. 2 a, b). Two Tule Technologies Inc. (Davis, CA, USA) (https://tule.ag/sensors/) evapotranspiration stations were installed in the field, one in check 9 which was a winter flooded treatment, and the other in check 6 where there was no winter flooding applied. This technology is based on the surface renewal method, which is returned to the customer as in-field daily evapotranspiration, ET_a. Watermark soil moisture sensors (https://irrometer.com) were installed in each plot (check) at four depths (30, 60, 90, and 120 cm) to monitor soil matric potential. The soil matric potential (SMP) in KPa was chosen and measured using the Watermarks since it represents the relative availability of the amount of water held in the soil profile for plant uptake than choosing the volumetric soil water content (SWC) which indicates the quantity of the water in the soil but does not directly indicate the availability of this water to plants.

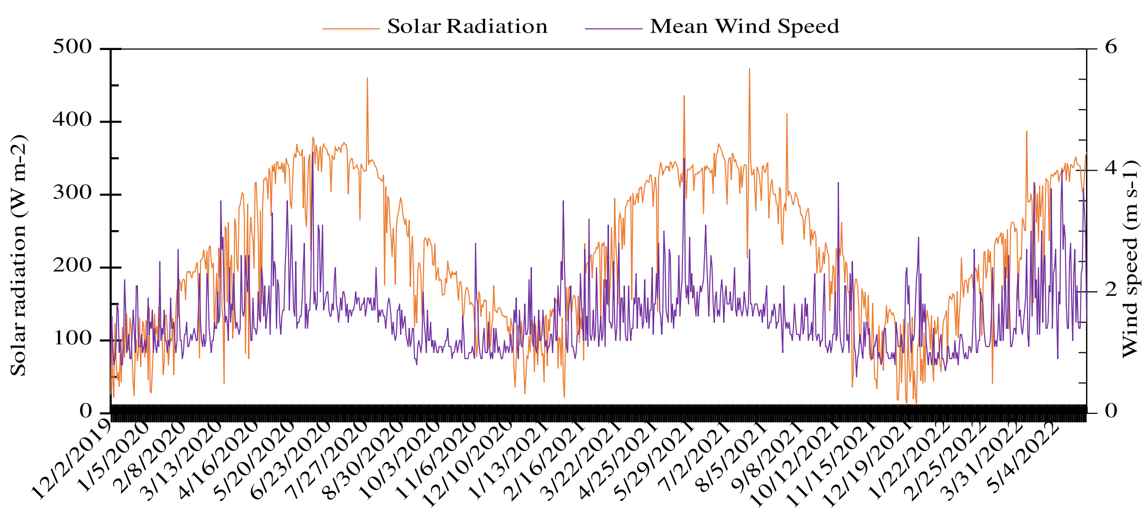

(a)

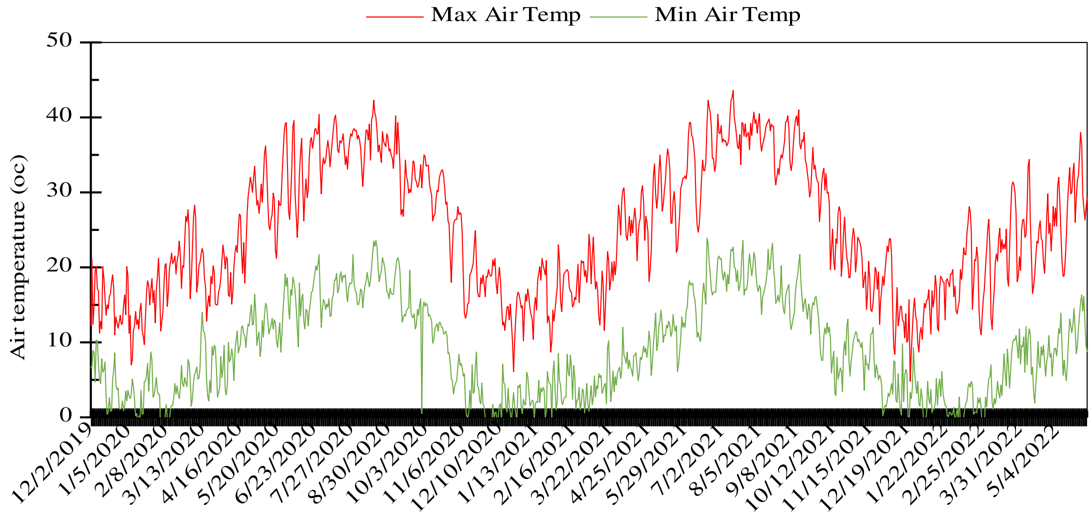

(b)

Fig. 2 (a) Solar radiation and mean wind speed **(b)** maximum and minimum air temperature

In the winters of 2020, 2021, and 2022 water was applied for groundwater recharge in the winter flooding treatments (Fig. 3, Table 1). The winter flooding of 2020 occurred from 20th February until 2nd April, resulting in 43 days of 10 intermittent flooding events with approximately one flooding event per week. In 2021, the winter flooding events occurred over 53 days, from 9th February to 2nd April, and consisted of 16 flooding events (approximately two flooding events/week). The third winter flooding (in 2022) was conducted from 20th January to 7th April, with 12 flooding events applied over 78 days (approximately one flooding event/week). Water for groundwater recharge was applied in addition to winter precipitation. Soil samples were collected before and after flooding events to develop the soil moisture retention curve (Fig. 4). In general, there is no specific trendline of the relation between the soil matric potential and the volumetric water content throughout the whole range of the volumetric water contents but could be specified in parts of the relationship. In the last segment of the trendline at the lower values of volumetric soil water content (near or below the wilting point), the relation could be linear which is similar to the Van Genuchten model (van Genuchten, 1980). The R^2 of the generated polynomial equation equals 0.95, and the equation was then used to calculate the volumetric water contents from the measured soil water potentials (Fig. 5 a– f). Later in the simulation, Van Genuchten–Mualem model was selected as a single–porosity model for defining soil hydraulic model without hysteresis. However, in practice, selecting the preferential flow model and fitting a perfect link between laboratory or theoretical model and field conditions is relatively difficult (Šimůnek *et al.*, 2003).

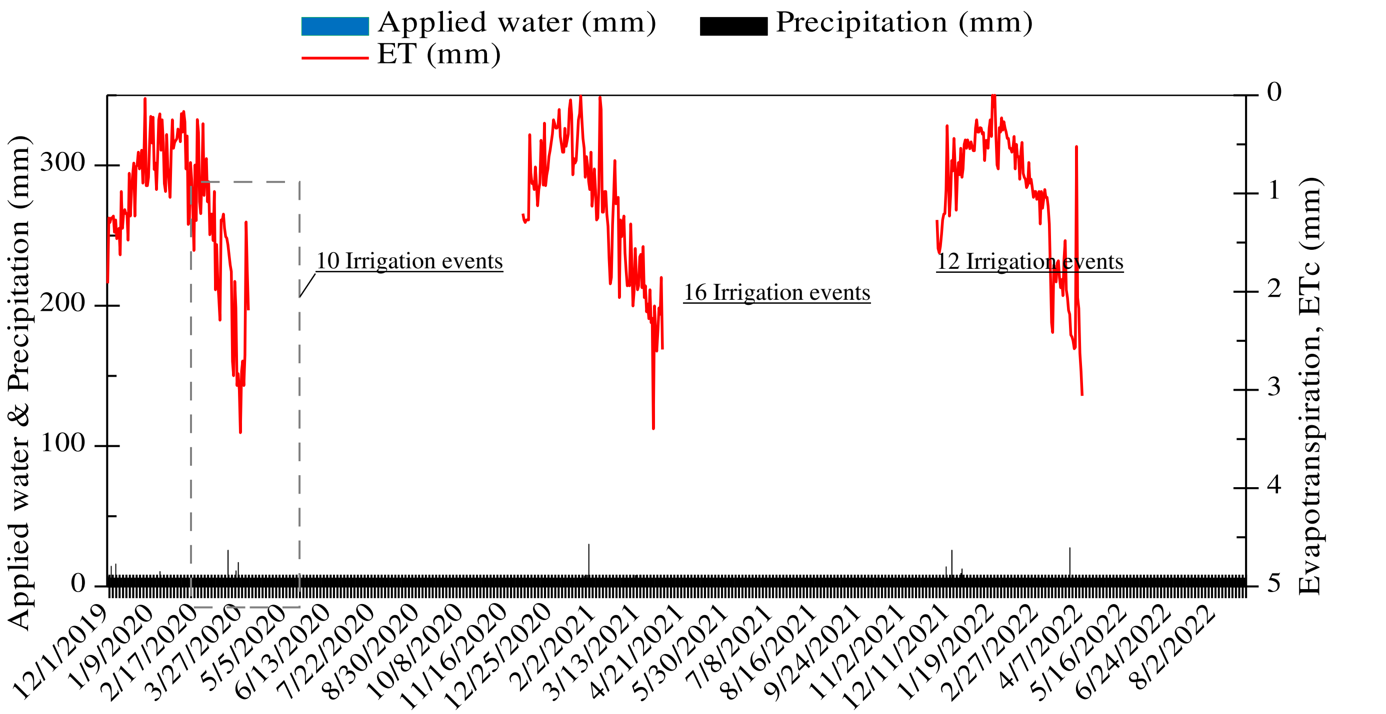

Fig. 3 Evapotranspiration (mm), precipitation (mm), and the applied winter flooding events (mm day^{-1}) during the 43, 53, and 78 days of 2020, 2021, and 2022, respectively

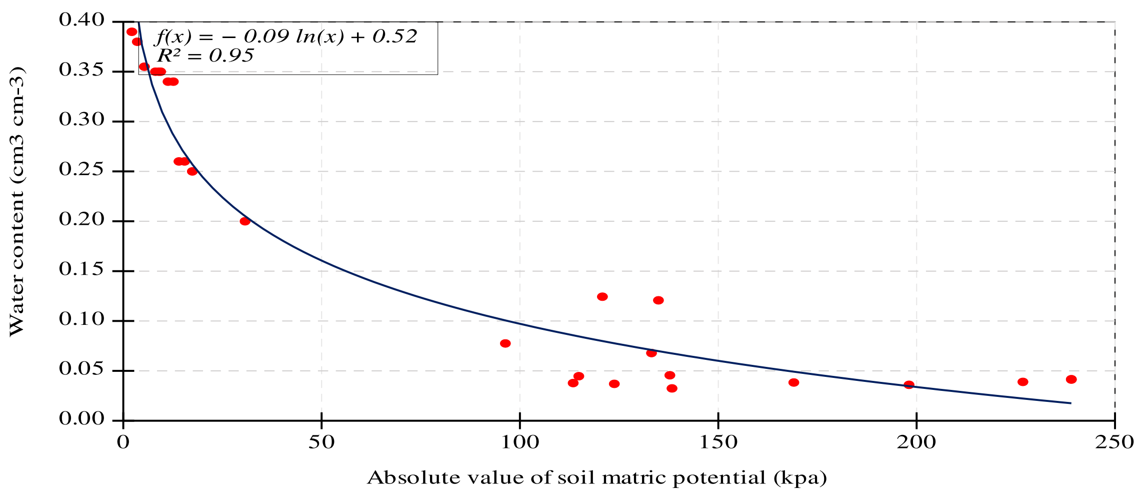

Fig. 4 Soil moisture retention curve for the sandy loam soil of the experimental study site

Table 1 Summary of the winter flooding events: dates and application amounts (in mm) during 2020, 2021, and 2022

	Date	Applied (mm)		Date	Applied (mm)		Date	Applied (mm)
							20 Jan	152
							27 Jan	190
							3 Feb	162
				9 Feb	101			
							10 Feb	126
				12 Feb	155			
				16 Feb	142			
							17 Feb	120
				19 Feb	106			
	20 Feb	116						
				23 Feb	131			
							24 Feb	156

winter floo	27 Feb	261	winter floo	26 Feb	113	winter floo	3 Mar	126
	5 Mar	288		2 Mar	119		10 Mar	138
	12 Mar	246		5 Mar	124		17 Mar	137
	17 Mar	145		9 Mar	120		24 Mar	148
	19 Mar	113		12 Mar	119		31 Mar	89
	23 Mar	141		16 Mar	119		7 Apr	138
	26 Mar	136		19 Mar	101			
	30 Mar	146		23 Mar	104			
	2 Apr	123		26 Mar	101			
				30 Mar	121			
				2 Apr	120			
Total		**1715**	**Total**		**1896**	**Total**		**1682**

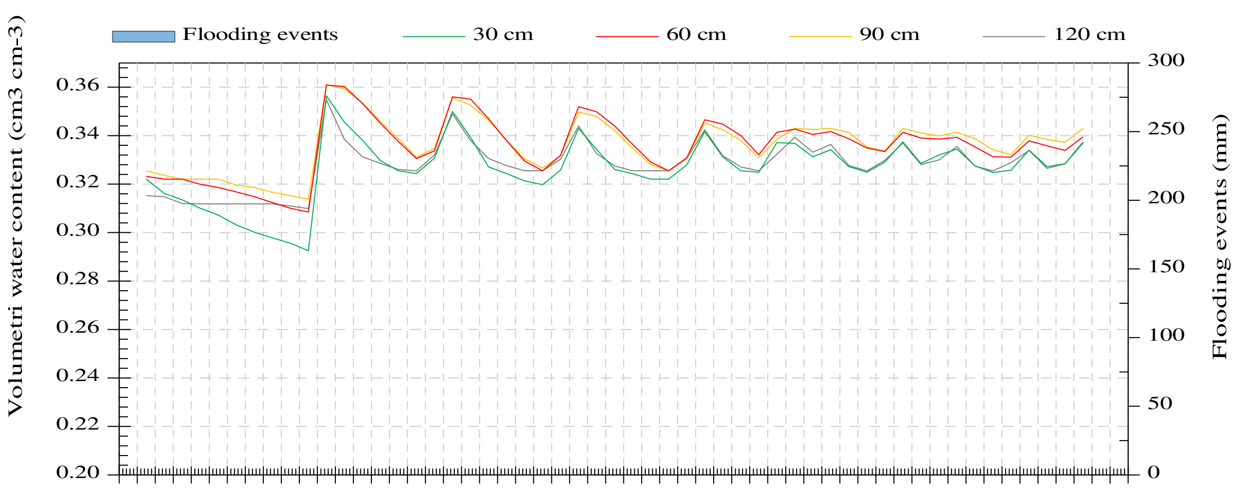

(a)

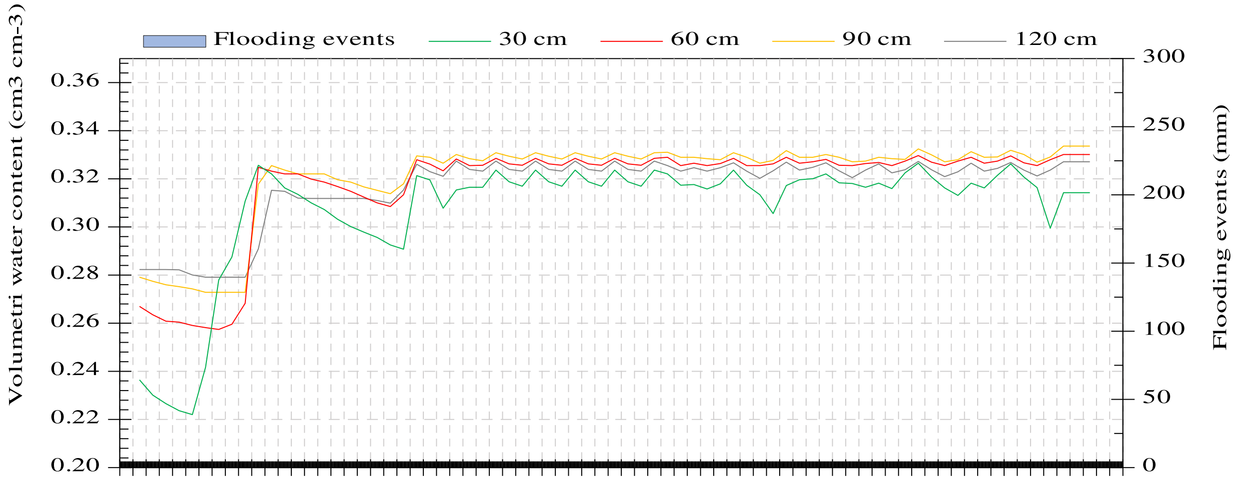

Flooding events
30 cm
60 cm
90 cm
120 cm
Volumetri water content (cm3 cm-3)
Flooding events (mm)
0.36
0.34
0.32
0.30
0.28
0.26
0.24
0.22
0.20
300
250
200
150
100
50
0

(b)

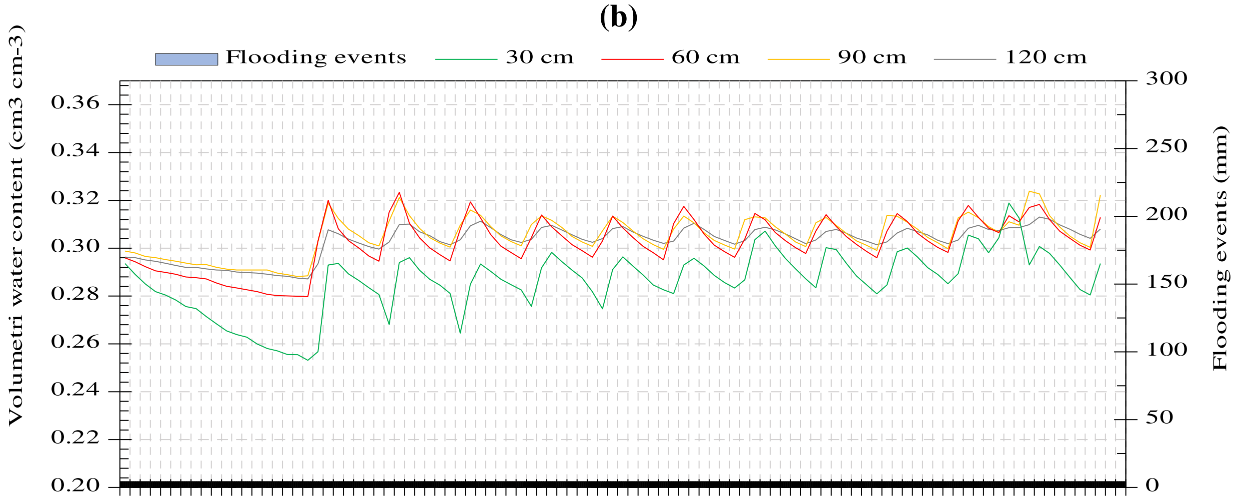

Flooding events
30 cm
60 cm
90 cm
120 cm
Volumetri water content (cm3 cm-3)
Flooding events (mm)
0.36
0.34
0.32
0.30
0.28
0.26
0.24
0.22
0.20
300
250
200
150
100
50
0

(c)

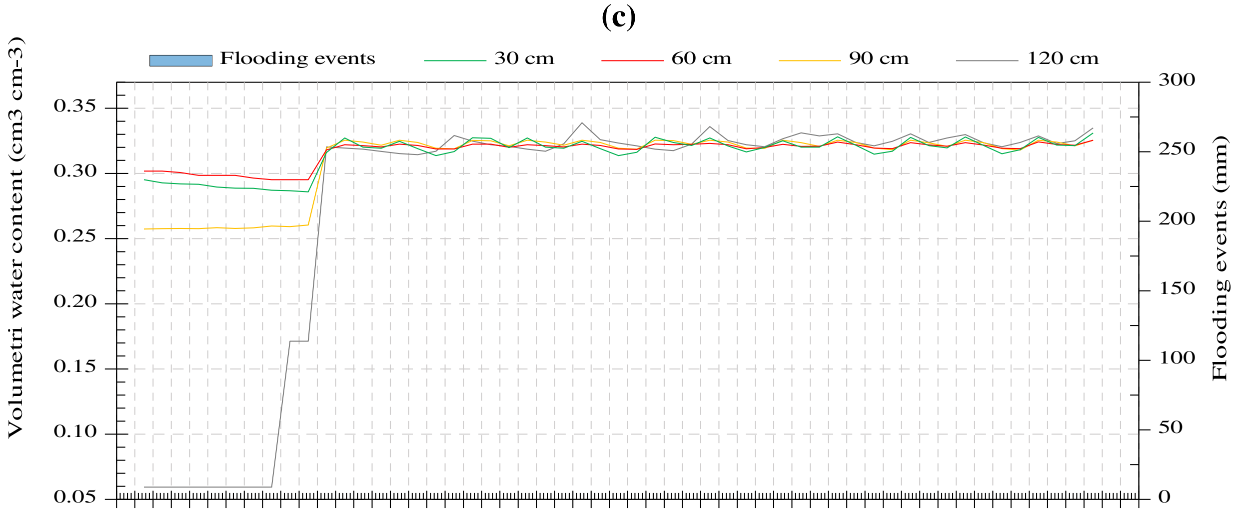

Flooding events
30 cm
60 cm
90 cm
120 cm
Volumetri water content (cm3 cm-3)
Flooding events (mm)
0.35
0.30
0.25
0.20
0.15
0.10
0.05
300
250
200
150
100
50
0

(d)

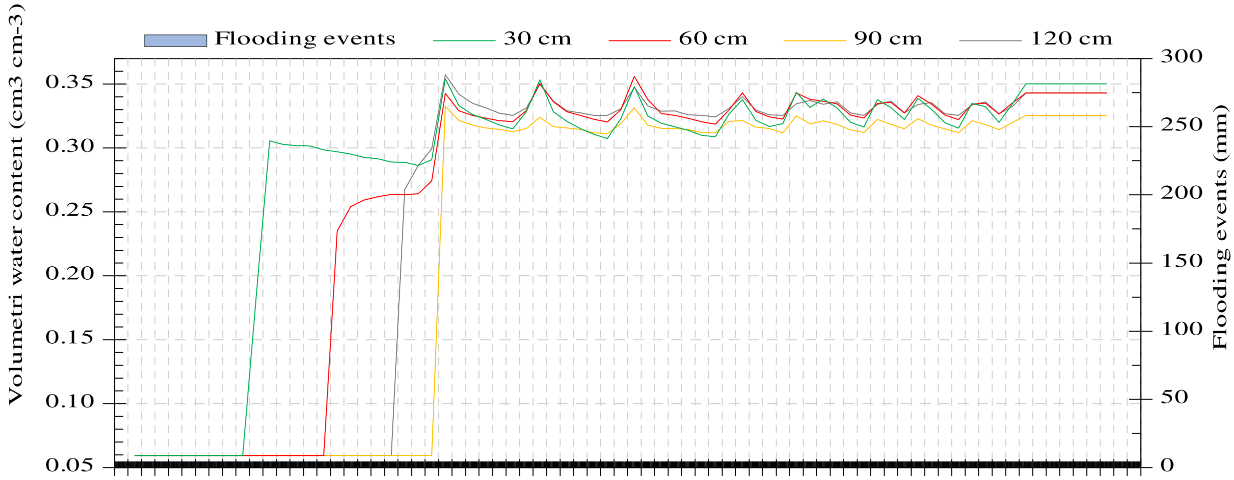

(e)

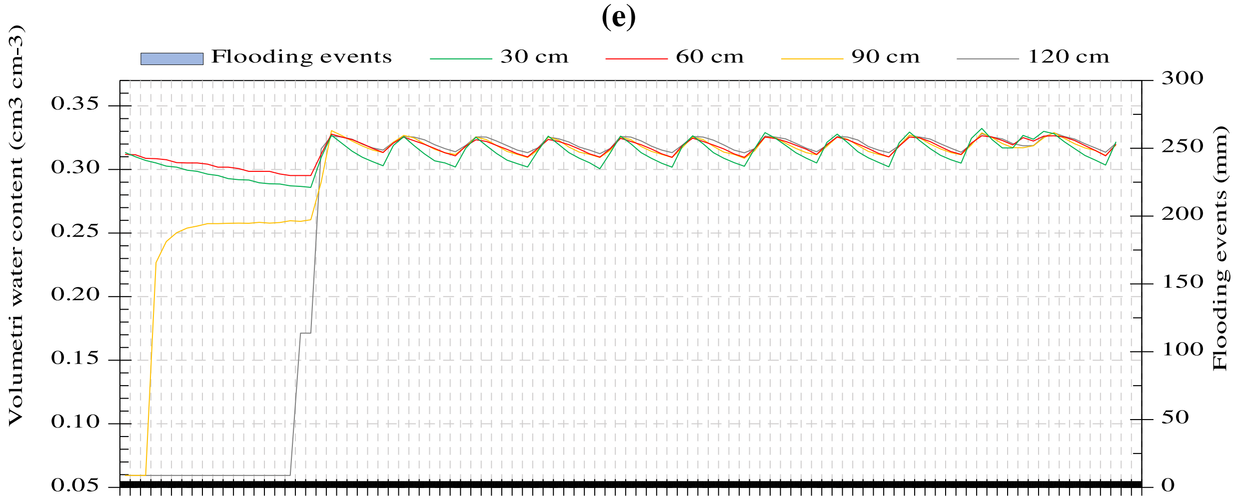

(f)

Fig. 5 Volumetric water content (θ, cm^3 cm^{-3}) measured at four depths during winter flooding following the fully irrigated treatment for **(a)** 2020, **(b)** 2021, and **(c)** 2022, respectively, and during the winter flooding following the mid-summer deficit irrigated treatment **(d)** 2020, **(e)** 2021, and **(f)** 2022

2.3. Numerical Simulation Model

2.3.1. Governing equations

HYDRUS is a finite element model for simulating the movement of water, heat, and multiple solutes in variably saturated media (Šimůnek *et al*., 2005). Water flow is simulated using Richards equation (Šimůnek *et al*., 1996), which allows incorporating a sink term to account for water uptake by plant roots (Feddes *et al*. 1978). HYDRUS can handle flow regions delineated by irregular boundaries. The flow region itself may be composed of nonuniform soils having an arbitrary degree of local anisotropy (Wang *et al*. 1997). Flow and transport can occur in a horizontal or vertical plane or a three-dimensional region. The water flows part of the model can deal with (constant or time-varying) prescribed head and flux boundaries, as well as boundaries controlled by atmospheric conditions. Soil surface boundary conditions may change during the simulation from prescribed flux to head-type conditions (and vice versa). In this study, we used HYDRUS-2D to numerically solve Richards' equation for the transient water flow through a homogeneous, isotopic soil (Šimůnek *et al*., 2008):

$$\frac{\partial\theta}{\partial t}=\frac{\partial}{\partial x}\left[\left(k(h)\frac{\partial h}{\partial x}\right)\right]+\frac{\partial}{\partial z}\left[\left(k(h)\frac{\partial h}{\partial z}\right)+k(h)\right]-S \quad (1)$$

Where θ is the volumetric water content [$L^3\,L^{-3}$], h is the soil-water pressure head [L], S is the sink source of water [T^{-1}], t is time [T], z is the vertical spatial coordinate of the simulated soil domain (depth) [L], and k is the hydraulic conductivity (LT^{-1}). The sink term (S) represents the volume of water removed per unit of time from a unit volume of soil due to plant water uptake. Feddes *et al*. (1978) defined S in terms of pressure head (h) to account for water stress:

$$S(h) = \alpha(h)\, S_p \quad (2)$$

Where the water stress function $\alpha(h)$ is dimensionless of the soil water pressure head ($0 \le \alpha \le 1$), and S_p is the potential water uptake rate [T^{-1}]. Water uptake is assumed to be zero close to saturation and below the wilting point pressure head. The spatial distribution of the roots can be specified using Vrugt model in HYDRUS simulation (Vrugt *et al*., 2001a, b). Solution of Eq. (1) requires characterization of the soil hydraulic properties, as defined by the soil water retention, $\theta(h)$, and unsaturated hydraulic conductivity function, $k(h)$. The constitutive relationships of van Genuchten-Mualem (van Genuchten, 1980) represent the effective saturation, S_e by:

$$S_e(h)=\frac{\theta-\theta_r}{\theta_s-\theta_r}=\frac{1}{[1+(-\alpha h)^n]^m} \quad (3)$$

and

$$k(h)=k_s S_e^l\left[1-\left(1-S_e^{\frac{1}{m}}\right)^m\right]^2 \quad (4)$$

Where θ is the volumetric water content [–], θ_s is the saturated water content [–], θ_r is the residual water content [–], $k(h)$ is the hydraulic conductivity in the matric potential (m) (pressure head), α [L^{-1}], k_s is the hydraulic conductivity in saturated conditions. n, l are shape parameters, and $m=1-\frac{1}{n}$. Though these four parameters are directly related to pore size distribution, pore connectivity, and tortuosity.

2.3.2. Boundary and initial conditions

HYDRUS-2D simulation requires setting boundary conditions along all the outer edges of the flow domain. In our study, the simulated domain has dimensions of 100 cm width and 120 cm depth (Fig. 6 a). A 5-cm mesh size was selected and the ratio of the sizes of two neighboring elements was restricted not to exceed 1.5. The vertical boundaries were assigned as no flux boundary, where one of them is due to symmetry, and the other due to the large extent of the computational domain. The top surface boundary was assigned as atmospheric pressure which allows for evaporation and transpiration to take place. Tule Technologies provided the daily *ETa* that was used as an input in the HYDRUS model and considered as "potential root water uptake (RWU)" for model simulation, then obtained the "actual" RWU.

A variable flux (Var.Fl_1, cm day^{-1}) was assigned along the top width (100 cm) of the domain on days when water was applied and the flux was set to zero on the day after, to swiftly change between the start and the end of the flooding event so that numerical coverage could be achieved without errors. Transpiration was assigned along the 100 cm top width. Groundwater was relatively deep (about 26 m away from the bottom boundary of the model domain) thus, the bottom boundary was assigned as free drainage along the whole bottom width (100 cm), thus the calculated flux (in cm^2 day^{-1}) would be divided by the 100 cm and multiplied by 10 to obtain how much water (in mm) per day seeped down for groundwater recharge.

Root distribution parameters are shown in Fig. 6b. The default iteration criteria and time discretization of HYDRUS-2D were used, except for the smaller initial time step (10^{-4} days) to overcome any potential convergence issues during infiltration. From the continuous monitoring of soil matric potential using Watermark sensors, volumetric water contents were calculated (using the soil moisture retention equation discussed earlier). The initial soil moisture at the beginning of simulation period of each year was clearly defined, and in this case, a warmup period was not assigned in the model simulation.

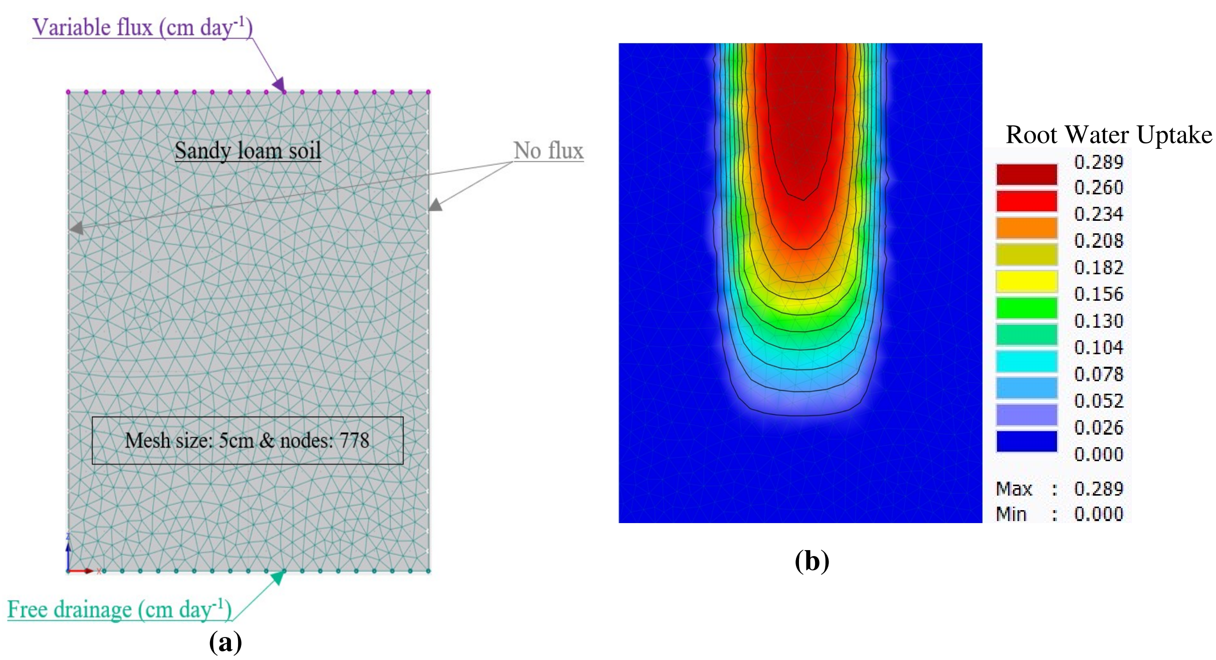

Fig. 6 **(a)** Conceptual model of the simulated domain where the soil is a uniform and isotropic sandy loam **(b)** Root distribution parameters

Initial soil moisture contents (θ_i) were calculated by converting soil matric potential, and kPa reading from Watermark sensors to volumetric water contents (cm^3 cm^{-3}) (along the soil profile) during a precedent period (a week to ten days) before starting the winter flooding events (for the two cases of the full (Fig. 5 a–c) and summer-deficit irrigation treatments (Fig. 5 d–f), for each year, 2020, 2021, and 2022. For the case of winter flooding after the full irrigation treatment, the soil moisture content was almost uniform along the soil depth where it ranged from 0.270 cm^3 cm^{-3} (at the top), to 0.280 cm^3 cm^{-3} (at the bottom), from 0.300 cm^3 cm^{-3} (at the top) to 0.310 cm^3 cm^{-3} (at the bottom), and from 0.258 cm^3 cm^{-3} (at the top) to 0.289 cm^3 cm^{-3} (at the bottom) for 2020, 2021, and 2022, respectively (Fig. 7 a–c). There were considerable spatial differences in the initial soil moisture values along the soil depth for the winter flooding treatments following the mid-summer deficit irrigation treatment. Values range from 0.180 cm^3 cm^{-3} (at the top) to 0.060 cm^3 cm^{-3} (at the bottom), from 0.295 cm^3 cm^{-3} (at the top) to 0.059 cm^3 cm^{-3} (at the bottom), and from 0.298 cm^3 cm^{-3} (at the top) to 0.059 cm^3 cm^{-3} (at the bottom) for the year 2020, 2021, and 2022, respectively (Fig. 7 d–f).

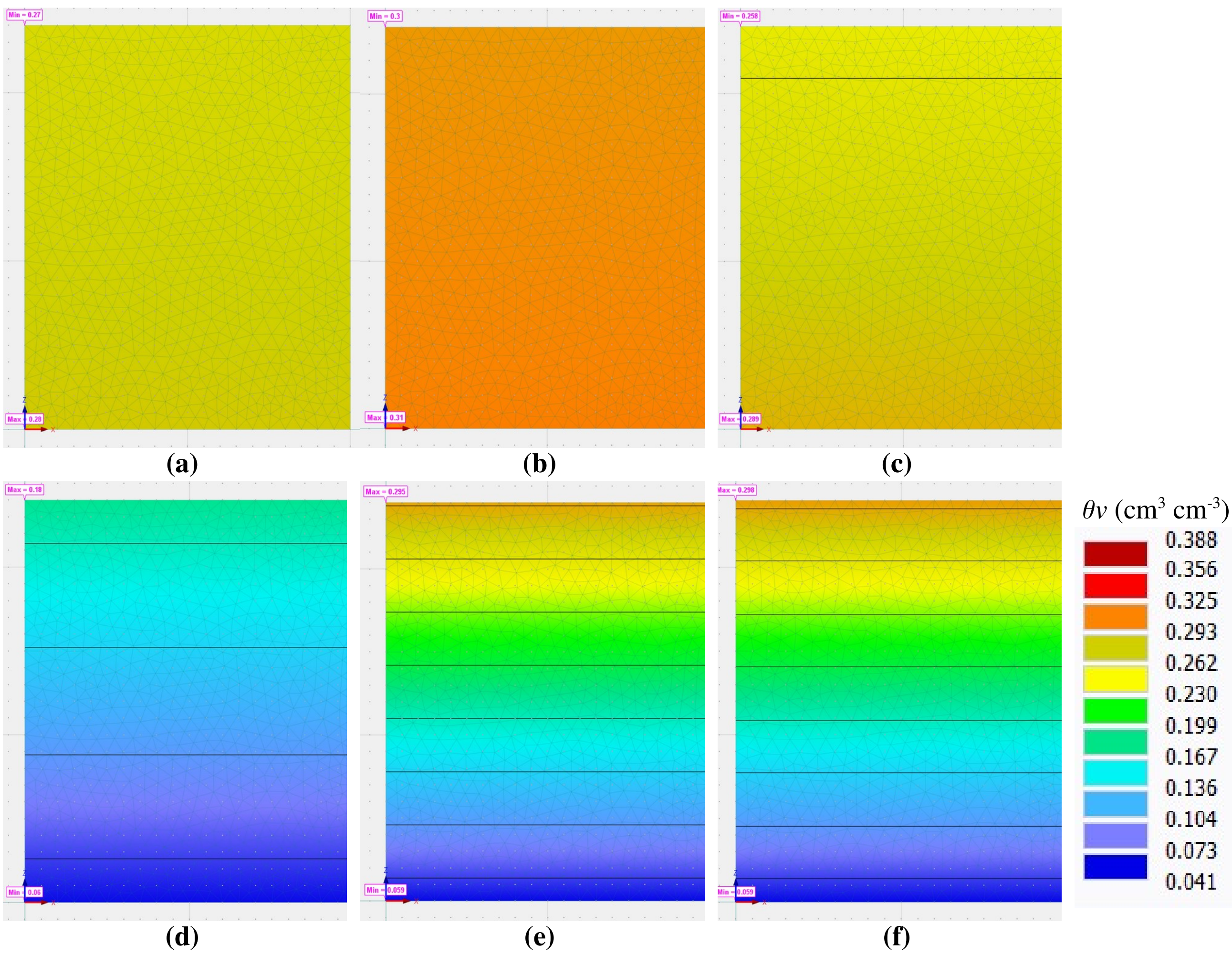

Fig. 7 Initial soil moisture contents (cm^3 cm^{-3}) at the beginning of the winter flooding along the soil profile (black lines are the edges between a smoothed colored scale of θv) for the winter flooding seasons of **(a)** 2020, **(b)** 2021, **(c)** 2022,

following full irrigation treatment in summer and the winter flooding seasons of **(d)** 2020, **(e)** 2021, and **(f)** 2022, following mid-summer deficit irrigation treatments

2.3.3. Soil and root water uptake parameters

Soil hydraulic parameters are required to be assigned in HYDRUS for the selected material either using the van Genuchten–Mualem relationships (van Genuchten, 1980) for the predefined soil types or using the neural network prediction functions. Table 2 shows the soil hydraulic parameters, and root distribution parameters in addition to Feddes' parameters used for the model simulation where α, n, and l in HYDRUS are considered to be merely empirical coefficients affecting the shape of the hydraulic functions. Root distribution directly affects the water uptake and therefore the soil-moisture distribution (Hao *et al*., 2005). Although crop water requirements were relatively small during the winter (evapotranspiration, ET_a is relatively small in winter and during the groundwater recharge period), the variation of root distribution parameters did not considerably affect the root water uptake, especially in winter flooding simulation. Thus, the growth of roots was not considered during the winter flooding period, assuming that half growth is achieved before flooding.

Table 2. Material properties for water flow, Feddes' parameters for root water uptake, and root distribution parameters

USDA (texture)	**van Genuchten retention parameters**					
Sandy loam	Q_r [-]	Q_s [-]	α [1/cm]	n [-]	k_s [cm day^{-1}]	l [-]
	0.041	0.388	0.024	1.407	36.125	0.5
Feddes' parameters for root water uptake						
P_O [cm]	P_{Opt} [cm]	P_{2H} [cm]	P_{2L} [cm]	P_3 [cm]	r_{2H} [cm day^{-1}]	r_{2L} [cm day^{-1}]
-10	-25	-1500	-1500	-8000	0.50	0.10
Root distribution parameters						
Max. depth	Depth of max. intensity		Max. root radius	Radius of max. intensity	Pz	Px
100 cm	60 cm		25 cm	15 cm	1	1

Simulations were executed for the winter flooding of 2020, 2021, and 2022 (twice for each year, for the case of full and mid-summer deficit irrigation treatments), six in total. The time variable boundary conditions were the same for the full and deficit irrigation scenarios for each year, while the initial moisture contents were different (previously shown in Fig. 7 a–f). Forty-three, fifty-three, and seventy-eight days were assigned as a final time for the winter flooding season of year 2020, 2021, and 2022, respectively. A daily time interval was assigned to differentiate the values of drainage after each flooding event (irrigation applications) for each flooding season, separately. The following water balance components: soil water content, root water uptake, and boundary fluxes (the variable flux at the top boundary, representing the applied winter water, and the bottom flux for the free drainage to groundwater) were quantified within the model to estimate annual and seasonal effects of the winter ag-MAR and summer irrigation treatments on the overall water balance and the amount of groundwater recharge.

2.3.4. Water Balance Calculation

A water balance model in HYDRUS 3x was used to calculate the fraction of applied winter water moving to deep percolation or groundwater recharge which is quantified as the flux through the bottom boundary of the domain (free drainage). Deep percolation was estimated at a daily time step. Previous research used HYDRUS for mass balance estimates and proved its accuracy of calculations (e.g., Han *et al.*, 2015; Tonkul *et al.*, 2019; Er-Raki *et al.*, 2021). In this study, groundwater recharge (GWR) was also calculated using the following soil water balance equation:

$$GWR_t = I_t + P_t + ET_a - \Delta S_t - R_t \tag{5}$$

Where I_t is the amount of winter applied water (mm) at time t, P_t is precipitation (rainfall) (mm), ET_a is actual evapotranspiration (mm), ΔS the change in soil storage (mm) (dependent on the available water capacity (AWC) of the soil), and R_t is surface runoff (mm) which was considered to be negligible since all applied water infiltrated downward (no surface runoff). For each time step, I was calculated from the difference in flowmeter readings at the beginning and end of the flooding event divided by the application area (check's area). The mass balance for groundwater recharge was calculated on a daily time step based on the change in soil water content (storage, ΔS) and the amount of free drainage that occurred at the bottom of the domain (120 cm depth). Finally, the total average contributions of applied water for groundwater recharge were calculated and compared between the three winter flooding seasons.

3. Results and Discussion

3.1. Results of Summer Treatments before Winter Flooding Treatments

Before presenting the results from HYDRUS simulations and water balance calculations of the two different winter flooding treatments, the previous summer treatments were discussed to interpret the difference in soil moisture and storage before winter flooding treatments (either starting the flooding or no flooding). Table 3 summarizes the irrigation data and duration of the full and mid-summer deficit summer treatments and how much water was saved as a result of the mid-summer deficit irrigation treatments. Results showed that 44%, 41%, and 37% of irrigation water was saved when the mid-summer deficit irrigation was implemented in 2019, 2020, and 2021, respectively.

Alfalfa experienced water stress during the 2019 growing season before the implementation of the mid-summer deficit treatment in August 2019 until the day of the groundwater recharge on 19th February 2020 while the applied water of the full treatment during summer was enough to meet the crop water requirements of 1397 mm. The applied irrigation water during the 2020, and 2021 growing seasons up to the implementation of mid-summer deficit irrigation treatment was adequate to meet the crop's water requirements, while the full irrigation treatments received more water than the actual evapotranspiration. 1019 and 1064 mm of water was applied while ET_a was 1026, and 1048 mm, during the 2020, and 2021 seasons, respectively.

The applied water during the full irrigation treatments in summer (from 12th May to 2nd Nov 2020, and from 23rd April to 19th Oct 2021) was over the ET_a by 698, and 641 mm, respectively. Cumulative ET_a from 3rd April 2020 to the date of the last irrigation event of full treatment (2nd Nov 2020) was 940 mm while from 3rd April 2020 to 19th Oct 2021 was 975 mm. This means that the over-irrigation during these two summer seasons (for the full treatment) provided water in advance which was not fully stored in the root zone and was available for the plant for the upcoming uptake. Some water was released down below the root zone when soil moisture was over the field capacity thus, the soil moisture content "the initial" before the upcoming winter treatments (either flooded or without flooding) was much higher (almost equal to the field capacity) than those following the deficit treatment in summer.

Table 3 Summary of summer treatments data of irrigation events, duration, ET_a, and % saving of irrigation water of mid-summer deficit than full irrigation

Summer treatments								
Note	Treatment	Irrigation water				Evapotranspiration, ET_a		% Saving of irrigation water
		No.	First event	Last event	Cumulative applied (mm)	Cumulative (mm)	Period of calculation	
Before winter treatments of 2020	Full	12	10th May 2019	30th Oct 2019	1397	1336	From 1st Jan 2019 to 19th Feb 2020	
	Mid-summer Deficit	7	10th May 2019	8th Aug 2019	777			44
Before winter treatments of 2021	Full	14	12th May 2020	2nd Nov 2020	1724	1026	From 3rd April 2020 to 8th Feb 2021	
	Mid-summer Deficit	7	12th May 2020	10th Aug 2020	1019			41
Before winter treatments of 2022	Full	14	23rd April 2021	19th Oct 2021	1689	1048	From 3rd April 2021 to 19th Jan 2022	
	Mid-summer Deficit	8	23rd April 2021	26th Jul 2021	1064			37

- Evapotranspiration, ET_a was calculated for the period between the date of the day just after the last day of applying the previous winter flooding to the day before the first day of applying the next winter flooding in the following year.
- For ET_a during summer of 2019 (before winter treatments of 2020), the starting date of the period where the evapotranspiration was calculated was on 1st January, when there was no previous winter treatment.

3.2. Root Water uptake and cumulative fluxes

After the HYDRUS model was set up for the two summer irrigation treatments (full and mid-summer deficit) and the winter flooding for 2020-2022, results of the spatial distribution of moisture content were first evaluated and compared with the moisture records from the soil matric potential measurements (using the Watermark sensors) in each plot and treatment. Winter flooding plots that were fully irrigated in the summer before the winter recharge experiment (checks 1, 8, and 9) had high initial soil moisture contents (Fig 7 a–c: volumetric water content ranges from 0.26 to 0.31 $cm^3\ cm^{-3}$). In contrast, the previous mid-summer deficit irrigation treatment (in checks 4, 5, and 12) had a marked effect on the initial soil moisture conditions before imposing the winter flooding treatments (Fig 5 d–f). Thus, initial moisture content of winter flooding plots after the mid-summer deficit was almost close to the residual moisture of the sandy loam (0.041 $cm^3\ cm^{-3}$, Fig 7 d–f).

Irrespective of the recharge or irrigation treatment, the actual root water uptake was nearly similar to the potential root water uptake indicating the crop had no stress. The winter flooding plots received the same amount of applied water in winter regardless of whether they were deficit or fully irrigated treatments (Table 1). The actual root water uptakes in the winter flooding–deficit irrigation treatments were similar to the flooding treatments that were fully irrigated partially reflecting crops' semi-dormancy and overall lower water use, however, they fluctuated from one year to another. Root water uptakes are shown in Fig. 8 a–c for the winter flooding (after mid-summer deficit irrigation and full irrigation treatments) for all three years where the x-axis represents the dates of the winter seasons, and the y-axis represents the root water uptake (mm). Generally, an upward increase in flux was observed over time during the winter flooding (towards April) where evapotranspiration increases.

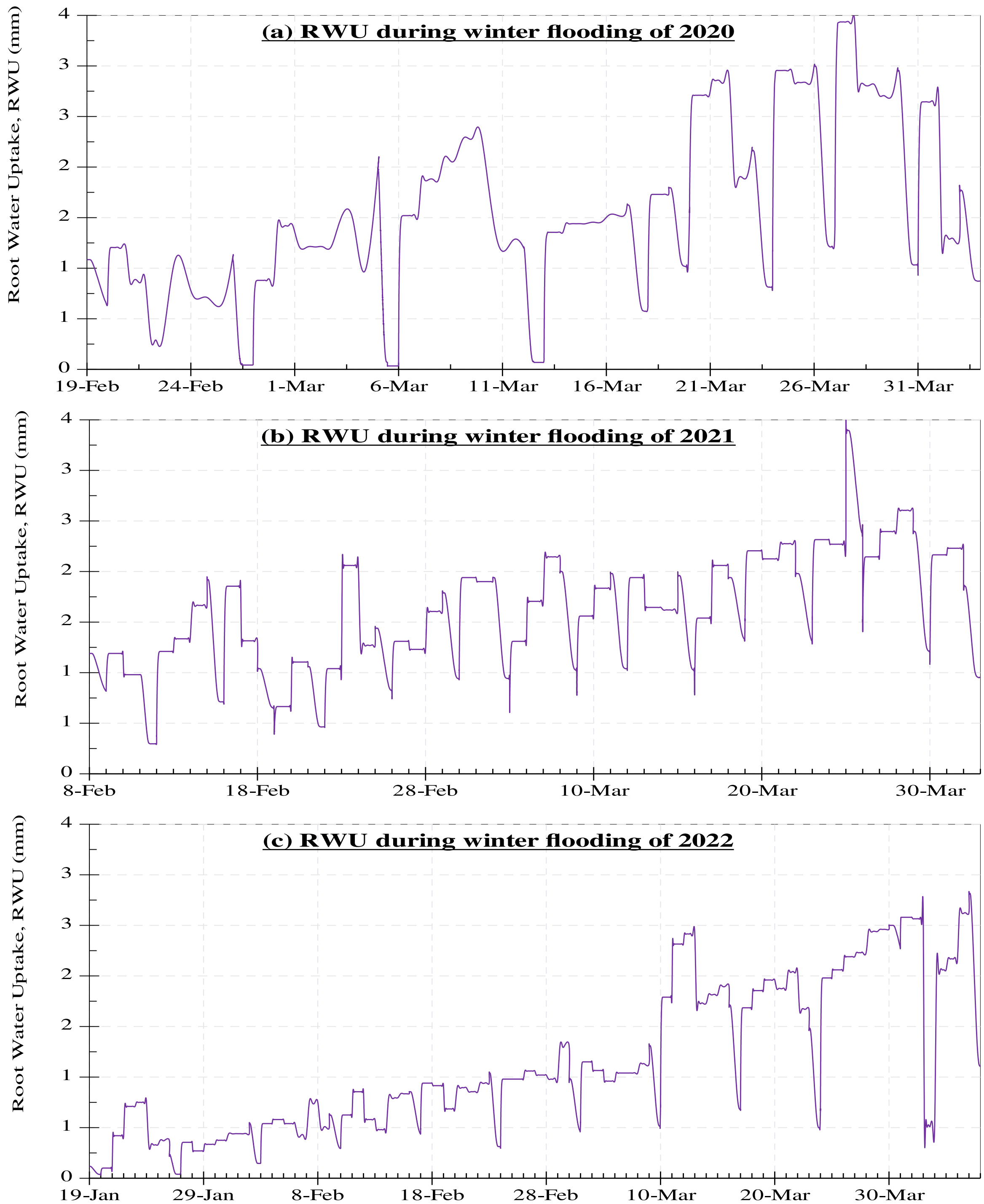

Fig. 8 Root water uptake (cm day^{-1}) during the winter flooding (either after full or mid-summer deficit irrigation treatments, where ET_a during the two summer treatments were the same) for **(a)** season of 2020, **(b)** season of 2021, and **(c)** season of 2022

Figs 9 a–c shows the cumulative root water uptake during the winter flooding season of 2020, 2021, and 2022. In all three seasons, almost all the applied water drained out of the bottom of the domain. The cumulative root water uptake recorded 66, 85, and 89 mm during the winter flooding of years 2020, 2021, and 2022, respectively for both the full and deficit irrigated treatments reflecting the expected minimal root water uptake due to minimal plant growth activity, and hence large flux of water towards the groundwater aquifer. The cumulative root water uptake was only 3.9, 4.5, and 5.3% of the cumulative applied water during the winter flooding periods in 2020, 2021, and 2022, respectively. Cumulative applied water during the winter flooding periods of 2020, 2021, and 2022 were 1715, 1896, and 1682 mm, respectively. In 2020, cumulative deep percolation of applied winter water was 1537 and 1366 mm for the full and mid-summer deficit irrigation treatments, respectively. In 2021, deep percolation of winter recharge was 1707 and 1577 mm for the full and mid-summer deficit treatments, respectively, and 1467, and 1391 mm in 2022 for the full and mid-summer deficit treatments, respectively.

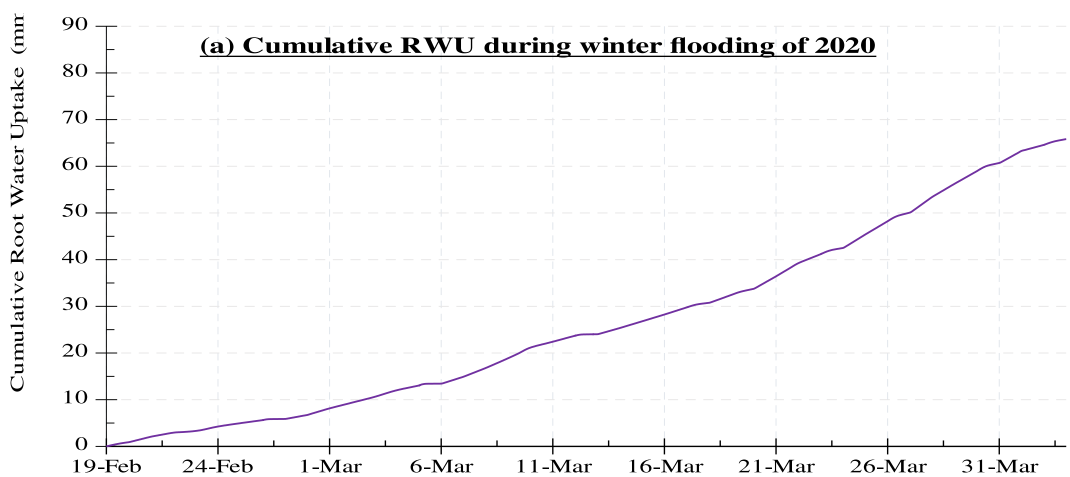

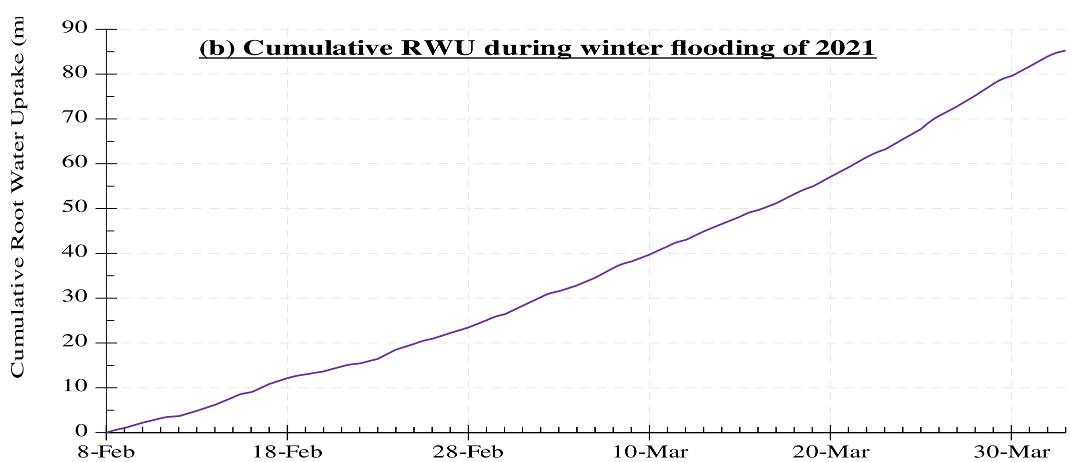

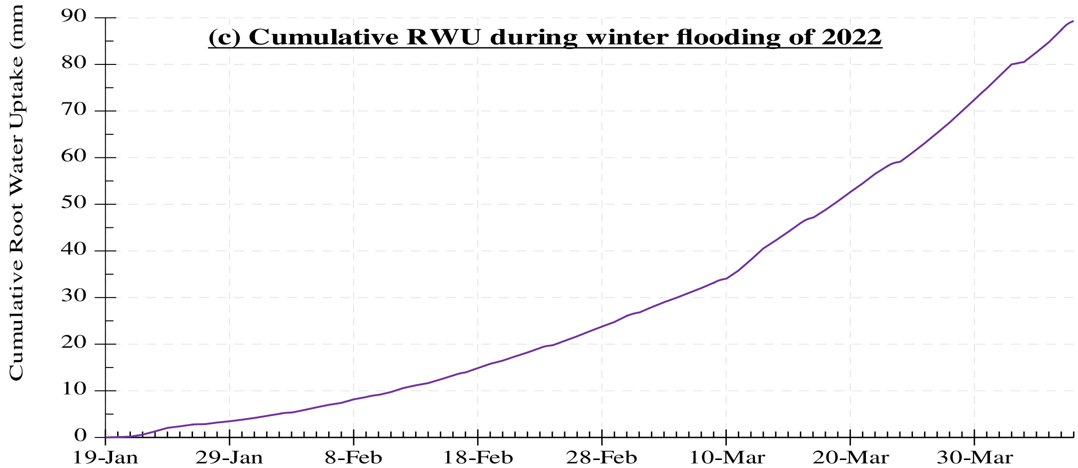

Fig. 9 Cumulative root water uptake (mm) for **(a)** winter flooding season of 2020 (43 days) full/deficit **(b)** for winter flooding season of 2021 (53 days) full/deficit **(c)** for winter flooding season of 2022 (78 days) full/deficit

3.3. Winter Flooding following Full-summer Irrigation Treatments

Free drainages (for recharging groundwater) were compared for the winter flooding seasons of 2020, 2021, and 2022 for the full irrigation treatment in summer. 2020, and 2022 have the same irrigation frequency (one irrigation event per week), and 2021 has two irrigation events per week. The comparison between the flooding frequency and the contribution to groundwater recharge was assessed over the three years, then the pattern of the free drainage was compared with the applied water events for each year (Fig. 10 a–c).

When winter flooding events were more frequent, more groundwater recharge was obtained while the total applied winter water was almost the same over the three years. Thus, the highest contribution to groundwater recharge was obtained in 2021 which was equal to 90.1% of the applied winter water. When one winter event per week was practiced, (for 2020, and 2022), the groundwater recharge was slightly lower, where it counted for 89.6% and 87.2% of the applied winter water, respectively. Table 4 summarizes the drainage and the applied water contribution to groundwater recharge for each flooding season.

Further, drainage pattern is associated with the winter events where drainage occurred after the application of each event, which is clearly shown as a sudden increase in the graph (Fig. 10 a–c). The number of drainage fluxes (pulses shown in Fig. 10 a–c) was equal to the number of winter irrigation events. Ten, sixteen, and twelve drainage fluxes were obtained during the flooding of 2020, 2021, and 2022, respectively, which are identical to the number of winter events. That means from the first applied irrigation event, drainage was observed across the bottom boundary. This is because the initial moisture content (right before applying the first flooding event) was close to the field capacity of the soil and this “additional water” brings the soil moisture to levels that exceeded its saturated capacity and then drainage started to occur.

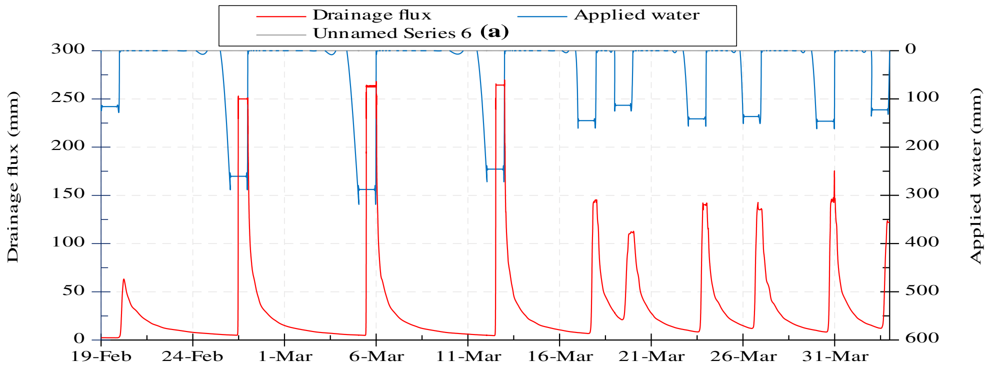
Drainage flux
Applied water
Unnamed Series 6
(a)
Drainage flux (mm)
Applied water (mm)
0
50
100
150
200
250
300
0
100
200
300
400
500
600
19-Feb
24-Feb
1-Mar
6-Mar
11-Mar
16-Mar
21-Mar
26-Mar
31-Mar

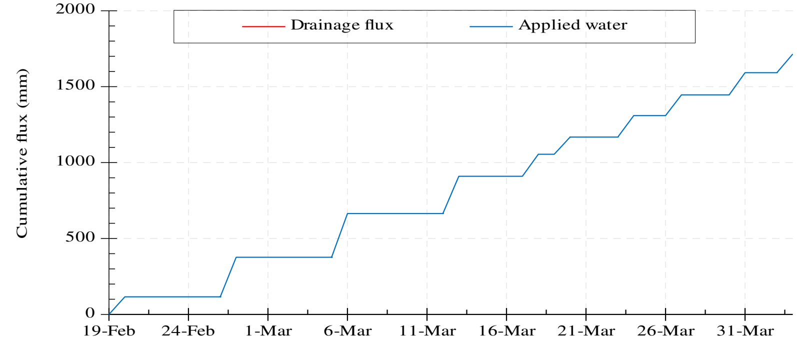
Drainage flux
Applied water
Cumulative flux (mm)
0
500
1000
1500
2000
19-Feb
24-Feb
1-Mar
6-Mar
11-Mar
16-Mar
21-Mar
26-Mar
31-Mar

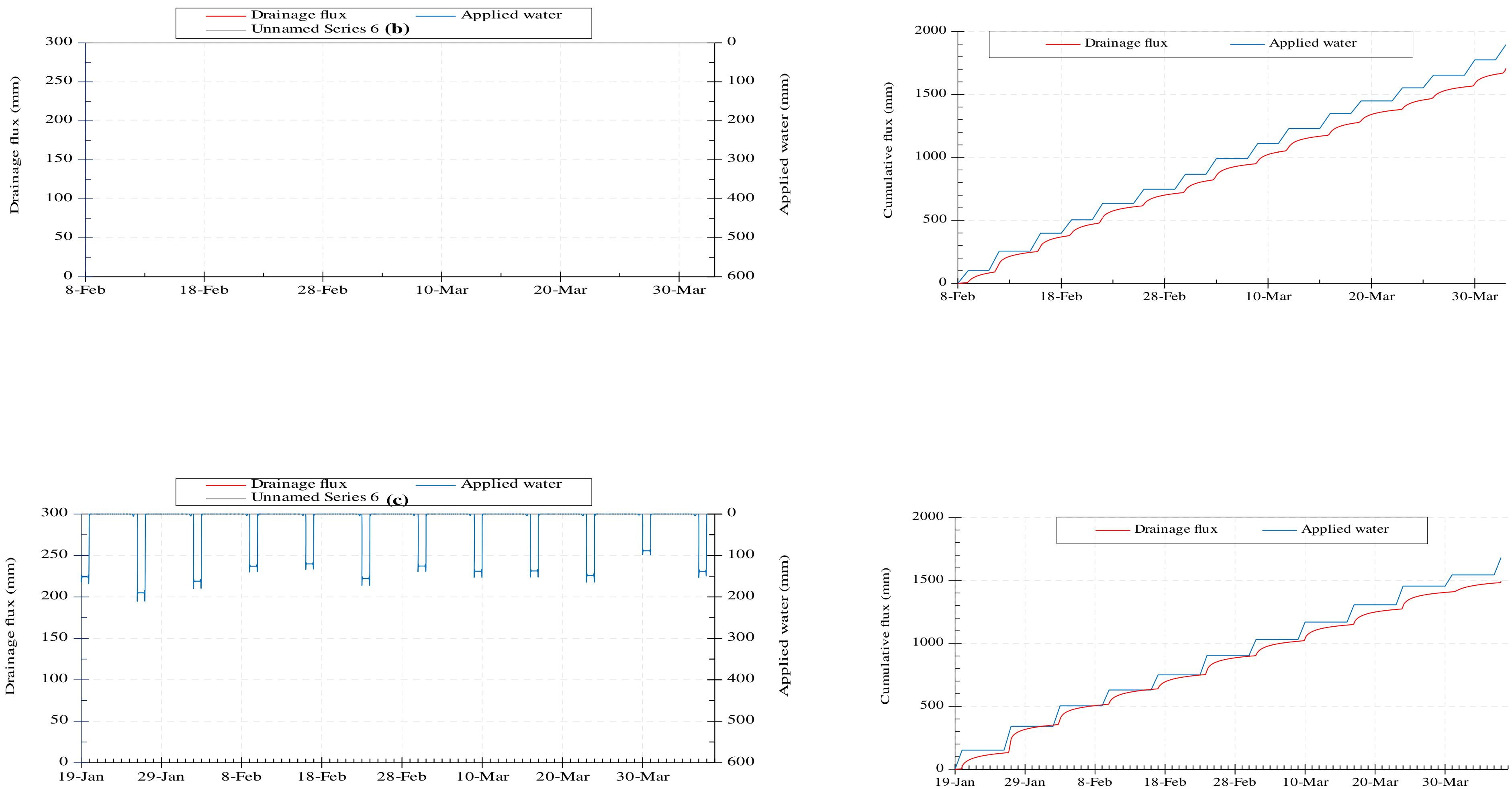

Fig. 10 Drainage (mm) and applied water (mm) during the winter flooding (left) and the cumulative fluxes (mm) (right) after full irrigation in summer growing seasons of **(a)** 2020, **(b)** 2021, and **(c)** 2022

Table 4 Applied water, groundwater recharge (in mm day^{-1}) just after each flooding event, and the percentage of groundwater recharge to the applied water during the winter flooding seasons following full irrigation treatment during the summer of 2020, 2021, and 2022.

2020																	
Flooding event	1st	2nd	3rd	4th	5th	6th	7th	8th	9th	10th							
Date	20 Feb	27 Feb	5 Mar	12 Mar	17 Mar	19 Mar	23 Mar	26 Mar	30 Mar	2 Apr							**Total**
No. of days (in simulation)	1	8	15	22	27	29	33	36	40	43							
Applied water, I_t (mm day^{-1})	116	261	288	246	145	113	141	136	146	123							1715
GW recharge, (mm/daily avg.)	63	248	259	231	133	101	130	125	135	112							1537
Percentage of GW recharge (%)	54	95	90	94	92	89	92	92	92	91							**90**
2021																	
Flooding event	1st	2nd	3rd	4th	5th	6th	7th	8th	9th	10th	11th	12th	13th	14th	15th	16th	**Total**
Date	9 Feb	12 Feb	16 Feb	19 Feb	23 Feb	26 Feb	2 Mar	5 Mar	9 Mar	12 Mar	16 Mar	19 Mar	23 Mar	26 Mar	30 Mar	2 Apr	
No. of days (in simulation)	1	4	8	11	14	18	22	25	29	32	36	39	43	46	50	53	
Applied water, I_t (mm day^{-1})	101	155	142	106	131	113	119	124	120	119	119	101	104	101	121	120	1896
GW recharge, (mm/daily avg.)	60	150	138	101	126	102	115	118	115	115	113	84	62	80	116	112	1707
Percentage of GW recharge (%)	59	97	97	95	96	90	97	95	96	97	95	83	60	79	96	93	**90**
2022																	
Flooding event	1st	2nd	3rd	4th	5th	6th	7th	8th	9th	10th	11th	12th					Total
Date	20 Jan	27 Jan	3 Feb	10 Feb	17 Feb	24 Feb	3 Mar	10 Mar	17 Mar	24 Mar	31 Mar	7 Apr					
No. of days (in simulation)	1	8	15	22	29	36	43	50	57	64	71	78					
Applied water, I_t (mm day^{-1})	152	190	162	126	120	156	126	138	137	148	89	138					1682
GW recharge, (mm/daily avg.)	146	182	140	107	101	136	119	120	120	130	32	134					1467
Percentage of GW recharge (%)	96	96	86	85	84	87	94	87	88	88	36	97					**87**

3.4. Winter Flooding following Mid-Summer Deficit Irrigation Treatment

Drainage fluxes of winter flooding after the mid-summer deficit irrigation treatments in 2020, 2021, and 2022 are shown in Fig. 11 a–c. Similar to winter flooding after the full irrigation treatment in summer, the highest contribution to groundwater recharge occurred when winter water was more frequent: two events per week than one event per week. The contribution of the applied winter water to groundwater recharge was 79.6%, 83.2%, and 82.7% for years 2020, 2021, and 2022, respectively (Table 5).

Regarding the drainage patterns for each year of flooding, it is clear that groundwater recharge did not occur from the beginning of the winter water application (Fig. 11 a–c). The first winter flooding event on the plots (4, 5, and 12) that were previously deficit irrigated during the summer had zero groundwater recharge. That means soil needs one full flooding event to bring the soil water content back to the field capacity or close to saturation. The drainage started to recharge the groundwater after the second winter event where it contributed to 86.4%, 96.7% from the second event of winter season of 2020, and 2022 while it counted for only 59.9% of the second water application for the frequently flooded events (season of 2021). Interestingly, for the third application event of the winter flooding season of 2021, the year with the more frequent applications, the contribution to groundwater recharge increased to 96.4%, around the values of the contribution from other consequent application events. This indicates that growers, who implement such practices, need to monitor the initial soil moisture content before starting the first flooding event to accurately estimate how much water is needed to bring the soil to saturation.

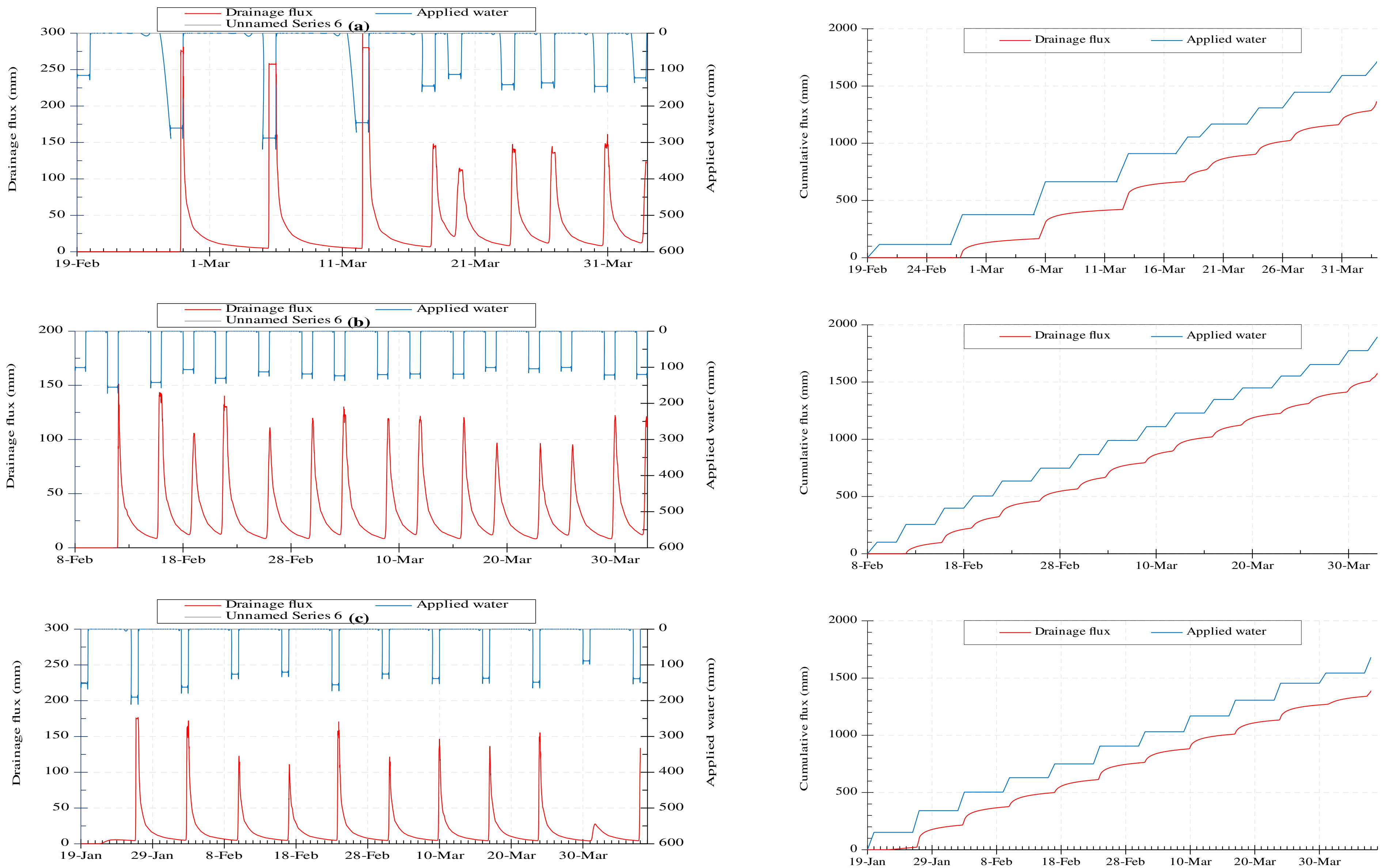

Fig. 11 Drainage (mm) and applied water (mm) during the winter flooding (left) and the cumulative fluxes (mm) (right) after deficit irrigation treatment in summer growing seasons of **(a)** 2020, **(b)** 2021, and **(c)** 2022

Table 5 Applied water, groundwater recharge (in mm day^{-1}) after each flooding event, and the percentage of groundwater recharge to the applied water during the winter flooding seasons following mid-summer deficit irrigation of the year 2020, 2021, and 2022.

							2020										
Flooding event	1st	2nd	3rd	4th	5th	6th	7th	8th	9th	10th							
Date	20 Feb	27 Feb	5 Mar	12 Mar	17 Mar	19 Mar	23 Mar	26 Mar	30 Mar	2 Apr							**Total**
No. of days (in simulation)	1	8	15	22	27	29	33	36	40	43							
Applied water, I_t (mm day^{-1})	116	261	288	246	145	113	141	136	146	123							1715
GW recharge, (mm/daily avg.)	0	225	232	226	124	101	120	118	118	102							1366
Percentage of GW recharge (%)	0.0	86	81	92	86	89	85	87	81	83							**80**
							2021										
Flooding event	1st	2nd	3rd	4th	5th	6th	7th	8th	9th	10th	11th	12th	13th	14th	15th	16th	
Date	9 Feb	12 Feb	16 Feb	19 Feb	23 Feb	26 Feb	2 Mar	5 Mar	9 Mar	12 Mar	16 Mar	19 Mar	23 Mar	26 Mar	30 Mar	2 Apr	**Total**
No. of days (in simulation)	1	4	8	11	14	18	22	25	29	32	36	39	43	46	50	53	
Applied water, I_t (mm day^{-1})	101	155	142	106	131	113	119	124	120	119	119	101	104	101	121	120	1896
GW recharge, (mm/daily avg.)	0	93	137	102	125	105	109	114	111	113	112	84	62	90	111	109	1577
Percentage of GW recharge (%)	0	60	96	96	95	93	92	92	93	95	94	83	**60**	89	92	91	**83**
							2022										
Flooding event	1st	2nd	3rd	4th	5th	6th	7th	8th	9th	10th	11th	12th					**Total**
Date	20 Jan	27 Jan	3 Feb	10 Feb	17 Feb	24 Feb	3 Mar	10 Mar	17 Mar	24 Mar	31 Mar	7 Apr					
No. of days (in simulation)	1	8	15	22	29	36	43	50	57	64	71	78					
Applied water, I_t (mm day^{-1})	152	190	162	126	120	156	126	138	137	148	89	138					1682
GW recharge, (mm/daily avg.)	0	184	160	110	111	143	117	135	133	147	25	126					1391
Percentage of GW recharge (%)	0.0	97	99	87	93	92	93	98	97	99	28	91					**83**

3.5. Water Balance

The water balance was calculated from daily soil moisture data and compared with HYDRUS simulation results for each winter flooding period. Table 6 summarizes these values and the contribution of applied water to the groundwater recharge after each flooding season. The total amount of groundwater recharge is mostly determined by the applied water through flooding events. It accounted for 85%, 89%, and 84% during the flooding seasons of 2020, 2021, and 2022, respectively after plots received the full irrigation treatment in summer. While for the winter flooding applied after deficit irrigation in summer, groundwater recharge accounted for only 78%, 79%, and 76% of the total applied water during winter flooding season of 2020, 2021, and 2022, respectively.

Since the experimental site had no significant precipitation during the flooding events and alfalfa was semi-dormant during winter flooding with minimal growth activity resulting in evapotranspiration amounting to 135, 150, and 186 mm during the winter flooding periods. These periods were from 20th February to 2nd April 2020, from 9th February to 2nd April 2021, and from 20th January to 7th April 2022. The total change in soil moisture (storage) during the three winter flooding seasons was considerably high when a previous deficit irrigation treatment was applied in summer compared to the full irrigation treatment. This indicates that initial soil moisture content was relatively low (near residual moisture content, θ_r) and more water was needed to fill soil storage in the deficit irrigated plots when applying winter water for Ag-MAR.

Generally, rainfall did not affect the total soil moisture in the entire soil profile before start of the winter seasons. The highest rainfall event prior to winter flooding (which started on 20th February) occurred on 16th January 2020 and accounted for 11 mm. A 31 mm of rainfall occurred on 28th January 2021, eleven days before the start of 2021 winter flooding season on 9th February. Small intermittent rainfall events took place between 1st January and 19th January 2022, 2 mm in total before starting winter flooding season of 2022 on 20th January.

The correlations between the observed values of the groundwater recharge (mm) and the calculated values from HYDRUS simulation after each flooding event of the three flooding periods (10, 16, and 12 events in 2020, 2021, and 2022) are shown in Fig. 12 a, and b. A very good agreement between HYDRUS results and the calculated values of groundwater recharge was obtained for the full and mid-summer deficit irrigation scenarios with R^2 values of 0.91, and 0.89, respectively.

Table 6 Summary of the mass balance input parameters (precipitation and applied water), change in soil storage, and estimated drainage (groundwater recharge) and its contribution to the applied water for the winter flooding treatments after full irrigation in summer and mid-summer deficit irrigation for 2020, 2021, and 2022.

Year	Treatment	Applied water (mm)	Precipitation (mm)	ET_a (mm)	Change in soil moisture (mm)	GW recharge (mm)	Contribution to GW (%)	% Contribution (from HYDRUS)
2020	Flood/Full	1715	52	135	173	1459	**85**	90
	Flood/ Deficit	1715	52	135	295	1337	**78**	80
2021	Flood/Full	1896	28	150	87	1687	**89**	90
	Flood/ Deficit	1896	28	150	276	1498	**79**	83
2022	Flood/Full	1682	40	186	121	1415	**84**	87
	Flood/ Deficit	1682	40	186	264	1272	**76**	83

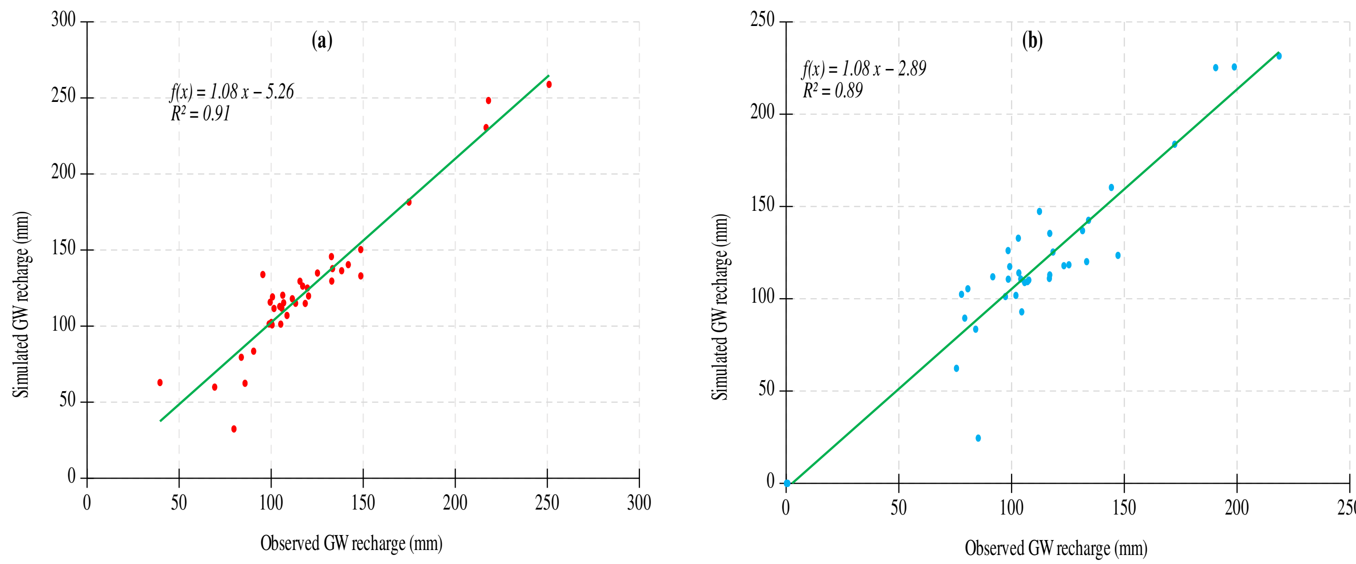

Fig. 12 Correlation between calculated and simulated groundwater (GW) recharge (mm) for **(a)** winter flooding after full irrigation treatment **(b)** winter flooding after mid-summer deficit treatment

4. Conclusion

The impact of different winter flooding and summer (full and deficit) irrigation treatments were investigated to quantify the potential of using alfalfa fields for groundwater recharge (also known as Ag-MAR) using field experimental data and HYDRUS-2D. The recharge was directly dependent on initial soil moisture content at the beginning of each winter flooding season as well as the water applied during the flooding season.

HYDRUS simulated recharge, root water uptake, evapotranspiration, and soil moisture dynamics well during winter flooding periods. For the winter flooding treatments that followed a full irrigation season, groundwater recharge amounts of 1537, 1707, and 1467 mm which is equivalent to 90, 90, and 87% of the applied water were achieved in 2020, 2021, and 2022, respectively. Recharge amounts during winter flooding following the mid-summer deficit irrigation treatment were 1366, 1577, and 1391 mm or 80, 83, and 83% of the applied water for years 2020, 2021, and 2022, respectively.

HYDRUS simulations agreed well (with R^2 values of 0.91, and 0.89 for winter flooding following full irrigation treatments, and winter flooding following deficit irrigation treatments, respectively) with calculated soil water balance estimates from field measurements. Results from this work demonstrate the importance of considering the initial soil moisture content prior to winter flooding for groundwater recharge as well as the benefits of starting the growing season with a full soil profile. Utilizing alfalfa fields and existing surface irrigation infrastructure could provide enough net recharge to meet the seasonal crop water requirements of alfalfa or other major crops in the San Joaquin Valley. While such groundwater recharge scenarios are possible during wet years, partial implementation of such practices could be utilized during most years when flooding events occur early in the year when most crops including alfalfa are dormant. The findings from this work could help growers, water regulators, and other stakeholders and policymakers in making informed decisions regarding sustainable water resources management in the San Joaquin Valley and other basins impacted by SGMA in California as well as other regions with similar agroecosystems.

Acknowledgments

Authors acknowledge the help from Staff Research Associates Brady Holder and Luke Paloutzian and UC– KARE support staff in the experimental setup and data collection. This work was supported by UC Kearney Agricultural Research and Extension Center and USDA-Agricultural Research Service (USDA–ARS) Collaborative Agreement No. 58-2034-8-038.

References

Alam S., Gebremichael M., Li R., Dozier J., Lettenmaier D.P. (2019) Climate change impacts on groundwater storage in the Central Valley, California. Climatic Change 157, 387–406, doi: 10.1007/s10584-019-02585-5

Bachand P.A., Roy S.B., Choperena J., Cameron D., Horwath W.R. (2014) Implications of using on-farm flood flow capture to recharge groundwater and mitigate flood risks along the Kings River, CA. Environmental science & technology 48, 13601–13609.

Dadgar M.A., Nakhaei M., Porhemmat J., Eliasi B., Biswas A. (2020) Potential groundwater recharge from deep drainage of irrigation water. Science of the Total Environment 716, 137105.

Dahlke H.E., Brown A.G., Orloff S., Putnam D., O'Geen T. (2018) Managed winter flooding of alfalfa recharges groundwater with minimal crop damage. California Agriculture 72, 65–75, doi: 10.3733/ca.2018a0001

DWR (2016) California's Groundwater Working Toward Sustainability Technical Report Bulletin 118, Department of Water Resources (DWR).

DWR (2017) Groundwater Level Change - Fall 2011 to Fall 2016. https://water.ca.gov/-/media/DWR-Website/Web-Pages/Programs/Groundwater-Management/Data-and-Tools/Files/Statewide-Reports/Groundwater-Conditions-Report-Fall-2021.pdf

Jasechko S., Perrone D. (2020) California's Central Valley Groundwater Wells Run Dry During Recent Drought. Earth's Future, 8 (4), e2019EF001339, doi: 10.1029/2019EF001339

Eltarabily M.G., Bali K.M., Negm A.M., Yoshimura C. (2019 a) Evaluation of root water uptake and urea fertigation distribution under subsurface drip irrigation. Water 11, 1487, doi: 10.3390/w11071487

Eltarabily M.G., Berndtsson R., Abdou N.M., El-Rawy M., Selim T. (2021) A comparative analysis of root growth modules in HYDRUS for SWC of rice under deficit drip irrigation. Water 13, 1892, doi: 10.3390/w13141892

Eltarabily M.G., Burke J.M., Bali K.M. (2019 b) Effect of deficit irrigation on nitrogen uptake of sunflower in the low desert region of California. Water 11, 2340, doi: 10.3390/w11112340

Er-Raki S., Ezzahar J., Merlin O., Amazirh A., Hssaine B.A., Kharrou M.H., Khabba S., Chehbouni A. (2021) Performance of the HYDRUS-1D model for water balance components assessment of irrigated winter wheat under different water managements in a semi-arid region of Morocco. Agricultural Water Management 244, 106546, doi: 10.1016/j.agwat.2020.106546

Feddes R.A., Kowalik P., Zarandy H. (1978) Simulation of Field Water Use and Crop Yield. Pudoc. Wageningen. The Netherlands Saline water in supplemental irrigation of wheat and barley under rainfed agriculture. Agricultural Water Management 78, 122–127

Ganot Y., Dahlke H.E. (2021 a) Natural and forced soil aeration during agricultural managed aquifer recharge. Vadose Zone Journal 20 (3), e20128, doi: 10.1002/ vzj2.20128.

Ganot Y., Dahlke H.E. (2021 b) A model for estimating Ag-MAR flooding duration based on crop tolerance, root depth, and soil texture data. Agricultural Water Management 255, 107031, doi: 10.1016/j.agwat.2021.107031

Han M., Zhao C. Šimůnek J., Feng G. (2015) Evaluating the impact of groundwater on cotton growth and root zone water balance using Hydrus-1D coupled with a crop growth model. Agricultural Water Management 160, 64–75, doi: 10.1016/j.agwat.2015.06.028

Hanak E., Lund J., Arnold B., Escriva-Bou A., Gray B., Green S., Harter T., Howitt R., MacEwan D., Medellín-Azuara J. (2017) Water stress and a changing San Joaquin Valley. Public Policy Institute of California 1, 5–48.

Hao X., Zhang R., Kravchenko A. (2005) Effects of root density distribution models on root water uptake and water flow under irrigation. Soil Science 170 (3), 167-174

https://cimis.water.ca.gov/Stations.aspx (accessed on 25 October 2022)

https://irrometer.com (accessed on 25 October 2022)

https://tule.ag/sensors/ (accessed on 25 October 2022)

https://water.ca.gov/programs/groundwater-management/sgma-groundwater-management (accessed on 25 October 2022)

https://websoilsurvey.sc.egov.usda.gov/App/WebSoilSurvey.aspx (accessed on 25 October 2022)

Jiménez-Martínez J., Skaggs T.H., van Genuchten M.T., Candela L. (2009) A root zone modelling approach to estimating groundwater recharge from irrigated areas. Journal of Hydrology 367, 138–149, 10.1016/j.jhydrol.2009.01.002

Kocis T.N., Dahlke H.E. (2017) Availability of high-magnitude streamflow for groundwater banking in the Central Valley, California. Environmental Research Letters 12, 084009, doi: 10.1088/1748-9326/aa7b1b

Levintal E., Kniffin M.L., Ganot Y., Marwaha N., Murphy N.P., Dahlke H.E. (2022) Agricultural managed aquifer recharge (Ag-MAR)—a method for sustainable groundwater management: A review. Critical Reviews in Environmental Science and Technology 1–24, doi: 10.1080/10643389.2022.2050160

Li B., Wang Y., Hill R.L., Li Z. (2019) Effects of apple orchards converted from farmlands on soil water balance in the deep loess deposits based on HYDRUS-1D model. Agriculture, Ecosystems & Environment 285, 106645, doi: 10.1016/j.agee.2019.106645

Li D. (2020) Quantifying water use and groundwater recharge under flood irrigation in an arid oasis of northwestern China. Agricultural Water Management 240, 106326.

Lu X., Jin M., van Genuchten M.T., Wang B. (2011) Groundwater recharge at five representative sites in the Hebei Plain, China. Groundwater 49, 286–294, doi: 10.1111/j.1745-6584.2009.00667.x

Lund J., Medellin-Azuara J., Durand J., Stone K. (2018) Lessons from California's 2012–2016 Drought. Journal of Water Resources Planning and Management, 144 (10), 04018067, doi: 10.1061/(ASCE)WR.1943-5452.0000984

National Agricultural Statistics Service (NASS). 2022. https://www.nass.usda.gov/

Niswonger R.G., Morway E.D., Triana E., Huntington J.L. (2017) Managed aquifer recharge through off-season irrigation in agricultural regions. Water Resources Research 53, 6970–6992, doi: 10.1002/2017WR020458

O'Geen A.T., Saal M.B., Dahlke H.E., Doll D.A., Elkins R.B., Fulton A., Fogg G.E., Harter T., Hopmans, J.W., Ingels C. (2015) Soil suitability index identifies potential areas for groundwater banking on agricultural lands. California Agriculture 69 (2), 75–84, doi: 10.3733/ca.v069n02p75

Patle G.T., Singh D.K., Sarangi A., Sahoo R.N. (2017) Modelling of groundwater recharge potential from irrigated paddy field under changing climate. Paddy and water environment 15, 413–423, doi: 10.1007/s10333-016-0559-6

Poch-Massegú R., Jiménez-Martínez J., Wallis K.J., de Cartagena F.R., Candela L. (2014) Irrigation return flow and nitrate leaching under different crops and irrigation methods in Western Mediterranean weather conditions. Agricultural Water Management 134, 1–13, doi: 10.1016/j.agwat.2013.11.017

Porhemmat J., Nakhaei M., Dadgar M.A., Biswas A. (2018) Investigating the effects of irrigation methods on potential groundwater recharge: A case study of semiarid regions in Iran. Journal of hydrology 565, 455–466, doi: 10.1016/j.jhydrol.2018.08.036

Post V.E.A., Zhou T., Neukum C. Koeniger P., Houben G.H., Lamparter A., Šimůnek J. (2022) Estimation of groundwater recharge rates using soil-water isotope profiles: a case study of two contrasting dune types on Langeoog Island, Germany. Hydrogeology Journal 30, 797–812, doi: 10.1007/s10040-022-02471-y

Putnam D.H., Montazar A., Bali K., Zaccaria D. (2015) Subsurface irrigation of alfalfa: benefits and pitfalls. In Proceedings, California Plant and Soil Conference California Chapter American Society of Agronomy Conference, Fresno, CA, USA. pp. 86-94. 4-5 February 2015, Fresno, CA. https://calasa.ucdavis.edu/Conference_Proceedings/

Putnam D.H. U. Gull and K. Bali. 2021. The Importance of Alfalfa in a Water-Challenged Future. In Proceedings, 2021 Western Alfalfa & Forage Symposium, Reno, NV 16-18, 2021. (http://alfalfa.ucdavis.edu) https://alfalfa.ucdavis.edu/+symposium/2021/index.aspx

Putnam D.H., and E. Lin. 2016. Nitrogen Dynamics in Cropping Systems – Why Alfalfa is Important. Pp. 423-49, IN Proceedings California Plant and Soil Conference. 2-3 February 2016. California Chapter American Society of Agronomy, Visalia, CA. https://calasa.ucdavis.edu/Conference_Proceedings/

Redfearn D. and B. Beckman, 2019. Reclaiming Flood Damaged Pastures and Forage Production. University of Nebraska Cooperative Extension. https://beef.unl.edu/beefwatch/reclaiming-flood-damaged-pastures-and-forage-production

Scanlon B.R., Healy R.W., Cook P.G. (2002) Choosing appropriate techniques for quantifying groundwater recharge. Hydrogeology Journal 10, 18–39, doi: 10.1007/s10040-001-0176-2

Šimůnek J. (2015) Estimating groundwater recharge using HYDRUS-1D. Engineering Geology and Hydrogeology 29, 25–36.

Šimůnek J., Jarvis N.J., Van Genuchten M.T., Gärdenäs A. (2003) Review and comparison of models for describing non-equilibrium and preferential flow and transport in the vadose zone. Journal of Hydrology 272, 14-35, doi: 10.1016/S0022-1694(02)00252-4

Šimůnek J., Šejna M., van Genuchten M.T. (1996) HYDRUS-2D: Simulating water flow and solute transport in two-dimensional variably saturated media. International Groundwater Modeling Center, Colorado School of Mines, Golden, Colorado.

Šimůnek J., van Genuchten M. T., Šejna M. (2005) The HYDRUS-1D software package for simulating the one-dimensional movement of water, heat, and multiple solutes in variably-saturated media. Version 3.0, HYDRUS Software Series 1, Department of Environmental Sciences, University of California Riverside, Riverside, CA, 270 pp

Šimůnek J., Van Genuchten M.T., Šejna M. (2008) Development and Applications of the HYDRUS and STANMOD Software Packages and Related Codes. Vadose Zone Journal 7 (2), 587–600, doi: 10.2136/vzj2007.0077

Stafford M.J., Hollander H.M., Dow K. (2022) Estimating groundwater recharge in the Assiniboine delta aquifer using HYDRUS-1D. Agricultural Water Management, 267, 107514, doi: 10.1016/j.agwat.2022.107514

Tonkul S., Baba A., Şimşek C., Durukan S., Demirkesen A.C., Tayfur G. (2019) Groundwater recharge estimation using HYDRUS 1D model in Alaşehir sub-basin of Gediz Basin in Turkey. Environmental Monitoring and Assessment 191, 610, doi: 10.1007/s10661-019-7792-6

USGS (United States Geological Survey) (2014) Water Use in the United States (US Department of the Interior, US Geological Survey)

Van Genuchten M.T. (1980) A Closed-form Equation for Predicting the Hydraulic Conductivity of Unsaturated Soils. Soil Science of American Journal 44 (5), 892–898, doi: 10.2136/sssaj1980.03615995004400050002x

Vrugt J.A., Hopmans J.W., Šimůnek J. (2001a) Calibration of a Two-Dimensional Root Water Uptake Model. Soil Science of American Journal 65 (4), 1027–1037, doi: 10.2136/sssaj2001.6541027x

Vrugt J.A., Van Wijk M.T., Hopmans W., Šimůnek J. (2001b) One-, two-, and three-dimensional root water uptake functions for transient modeling. Water Resources Research 37 (10), 2457–2470, doi: 10.1029/2000WR000027

Wang D., Yates S.R., Šimůnek J., van Genuchten M.T. (1997) Solute transport in simulated conductivity fields under different irrigations. *Journal of Irrigation and Drainage Engineering* 123(5), 336-343, doi: 10.1061/(ASCE)0733-9437(1997)123:5(336)

Wang W., Zhao J., Duan L. (2021) Simulation of irrigation-induced groundwater recharge in an arid area of China. Hydrogeology Journal 29, 525–540, doi: 10.1007/s10040-020-02270-3

Zhang Z., Wang W., Gong C., Zhang M. (2020) A comparison of methods to estimate groundwater recharge from bare soil based on data observed by a large-scale lysimeter. Hydrological Processes 34, 2987–2999, doi: 10.1002/hyp.13769